Combining EPS geofoam with geocells to reduce buried pipe loads and trench surface rutting

S.N. Moghaddas Tafreshi[1,*] (Corresponding Author), N. Joz Darabi[2], A.R. Dawson[3]

[1,*]*Corresponding Author. Professor, Department of Civil Engineering, K.N. Toosi University of Technology, Valiasr St., Mirdamad Cr., Tehran, Iran. Tel: +982188779473; Fax: +982188779476; E-mail address: nas_moghaddas@kntu.ac.ir*

[2]*PhD Candidate, Department of Civil Engineering, K.N. Toosi University of Technology, Valiasr St., Mirdamad Cr., Tehran, Iran. Tel: +982188779473; Fax: +982188779476; E-mail address: ndarabi@mail.kntu.ac.ir*

[3]*Associate Professor, Nottingham Transportation Engineering Centre, University of Nottingham, Nottingham, UK. Tel: +441159513902; Fax: +441159513909; E-mail address: andrew.dawson@nottingham.ac.uk*

Abstract:

This paper reports full scale experiments, under simulated heavy traffic, of geocell and EPS (expanded polystyrene) geofoam block inclusions to mitigate the pressure on, and deformation of, shallow buried, high density polyethylene (HDPE) flexible pipes while limiting surface settlement of the backfilled trench. Geocell of two pocket sizes and EPS of different widths and thickness are used. Soil surface settlement, pipe deformation and transferred pressure onto the pipe are evaluated under repeated loading. The results show that using EPS may sometimes lead to larger surface settlements but can alleviate pressure onto the pipe and, consequentially, result in lower pipe deformations. This benefit is enhanced by the use of geocell reinforcement which not only significantly opposes any EPS-induced increase in soil surface settlement, but further reduces the pressure on the pipe and its deformation to within allowable limits. For example, by using EPS geofoam with width 0.3 times, and thickness 1.5 times, pipe diameter simultaneously with geocell reinforcement with a pocket size 110×110 mm^2 soil surface settlement, pipe deformation and transferred pressure around a shallow pipe were respectively, 0.60, 0.52 and 0.46 times those obtained in the fully unreinforced buried pipe system. This would represent a desirable and allowable arrangement.

Keywords: *Geosynthetics, buried pipe, EPS block, geocell layer, pipe diameter change, pressure, soil surface settlement*

1. Introduction

The pressure acting on buried pipes is significantly influenced by relative settlements between soil prisms above and adjacent to the pipe. This relative settlement may have a positive or a negative influence on the pipe behaviour due to the phenomenon of arching (Marston and Anderson, 1913; Marston, 1930), inducing

shear stresses between the soil prisms above and adjacent to the pipe that may increase or decrease the load that reaches the pipe, whether it originates from the self-weight of overburden soil or from static and cyclic surface surcharge loadings.

For rigid pipes, the deformation of the pipe crown is generally insignificant and thus the settlement of the soil immediately above the pipe is less than that of the adjacent soil prisms. This differential settlement of the soil gives rise to a concentration of pressure on the pipe crown due to the downward shear stress generated on the central soil prism by the adjacent, settling, soil prisms, and is called the negative arching effect (Fig. 1).

For flexible pipes, due to the relatively large downward deflection of the pipe crown, the settlement of the central soil prism above the pipe can often be greater than that of the adjacent soil prisms and, consequently, the pressure acting on the pipe crown reduces as shear stress is mobilized when the adjacent soil prisms act to partially support the central soil prism; an effect called positive arching (Fig. 1).

Hence, in order to reduce the stress carried by the pipe, it may be desirable to induce more settlement in the central prism compared with the two adjacent prisms (i.e. to enhance positive arching). This may be encouraged by the use of compressible low-density material such as sawdust, leaves, wood waste, straw bales, compressive soil, polystyrene beads placed in the central prism, above the pipe, during trench installation (e.g. as suggested by McAfee and Valsangkar, 2004; Kang et al., 2008a,b). Due to their low density, overburden loading is reduced, while the greater compressibility can reduce deflection of the buried pipe by inducing upward shearing stress on the two sides of central soil prism.

McAffee and Valsangkar (2004) conducted a testing program using a large-scale consolidometer and direct shear testing apparatus, to measure the compressibility and shear strength parameters of compressible fill materials (e.g. sawdust, wood chips, and hay) commonly used in such an application. Kang et al. (2008b) investigated the potential benefits of soft/low-density material, with moduli of elasticity ranging from 345 kPa for polystyrene beads to 2756 kPa for bales of hay, and the optimum geometry of their use around the deeply buried pipe, using finite element model. They reported a reduction in the vertical pressure on the pipe crown due to this innovative extension of a narrow zone of the soft material.

Neither engineering properties, compaction, nor mechanical characteristics of these materials (sawdust, leaves, wood chips, straw bales and polystyrene beads) are commonly difficult to determine and control in principle although, usually, their uniformity when compacted in a trench, is not reliable. Amongst the low-density materials, expanded polystyrene (EPS) geofoam (available in block form) is more uniform with fairly reliable engineering properties and its stress-strain behaviour is controllable and predictable. Thus, the use of

expanded polystyrene (EPS) geofoam blocks as a compressible inclusion has sparked interest in several different geotechnical applications such as road embankments, reinforced walls, buried pipes and culverts (Duskov, 1997; Zou et al., 2000; Zarnani and Bathurst 2007; Farnsworth et al., 2008; Hatami and Witthoeft, 2008; Barrett and Valsangkar, 2009; Horvath, 2010; Newman et al., 2010; Bartlett et al., J. 2015; Witthoeft and Kim, 2015; Keller, 2016; Meguid et al., 2017a,b).

Several researchers have focused on the use of expanded polystyrene (EPS) geofoam as a compressible inclusion to protect buried pipes and culverts (e.g., Vaslestad et al. 1994; Sun et al. 2005, 2009; Kim et al. 2010; Witthoeft and Kim, 2015; Anil et al., 2015; Beju and Mandal, 2017). Sun et al. (2009) investigated the pressure reduction on concrete culverts with EPS panels in various configurations using both instrumented field tests and numerical analyses. Their results encouraged the use of EPS geofoam block to effectively reduce the vertical pressure on rigid culverts. To identify the applicability of such compressible inclusions, Kim et al. (2010) conducted a series of model tests on corrugated steel pipes with a diameter of 100 mm. The vertical pressure acting on the pipe crown under three static surcharges of 49, 98, and 147 kPa to the backfill surface was measured. The results revealed that the vertical pressure acting on the pipe covered by one layer of EPS geofoam panel with a thickness of 50 mm (0.5 times the pipe diameter) could reduce by up to 73%, at an optimal width of EPS panel which equalled 1.5 times the pipe diameter. Witthoeft and Kim (2015) performed a numerical analysis to study the benefit of expanded polystyrene (EPS) geofoam panels placed over a buried pipe under the same three static surcharges. They found that EPS geofoam panel as compressible inclusions over a buried pipe with thickness of 50 mm and width of 1.5 times the pipe diameter delivered the greatest effectiveness in reducing the pressure acting on the pipe due to positive arching action. Anil et al. (2015) investigated the benefit of EPS geofoam blocks, with thicknesses of 30 and 50 mm, to protect pipes with diameter of 220 mm, manufactured from steel and composite materials from sudden impact loads such as rock falls. Impact load and accelerations on the pipes with time were measured. Their findings show that the installation of 50 mm thick geofoam with 80 mm thick sand (as cover) was generally successful in reducing the effects of impact loads in terms of dissipating impact effects on the pipe and of the measured acceleration and displacements of the pipe.

Even though using EPS geofoam block as compressible inclusions over a buried pipe has been observed to reduce the vertical stress acting on the pipe, yet its effect on pipe deformation has not been clearly reported in the literature. Potentially, the use of an EPS block over a buried pipe could cause disadvantages like low

surface modulus of elasticity and high deformation of the central soil prism - consequently leading to an increase in the soil surface settlement. This has not, previously, been investigated.

Soil-filled geocells can provide a three-dimensional cellular reinforcement. Many authors (Dash et al., 2007; Madhavi Latha and Rajagopal, 2007; Leshchinsky and Ling, 2012, 2013; Tanyu et al., 2013; Moghaddas Tafreshi et al., 2013, 2016; Hegde and Sitharam, 2015a; Indraratna et al., 2015; Biabani et al., 2016; Trung Ngo et al., 2016; Oliaei and Kouzegaran, 2017; Dash and Choudhary, 2018; Satyal et al., 2018) have shown that a geocell layer, due to the frictional and passive resistance developed at the soil-geocell interfaces, appears to derive substantial anchorage from both sides of the loaded area and, as a result, decreases soil surface settlement and increases bearing capacity. Thus, the use of geocell reinforcement in the buried pipe system, beneath the loading surface might not only considerably negate the tendency of an EPS block to increase soil surface settlement, but it could also cause more reduction in the transferred pressure over the pipe. Other researchers have studied the potential use of EPS blocks on buried pipe, particularly under static loading (e.g. Vaslestad et al. 1994; Kim et al. 2010; Witthoeft and Kim, 2015; Beju and Mandal, 2017), and the geocell reinforcement of soil over pipes buried under rubber-soil mixtures and subjected to static and repeated loading (e.g. Tavakoli Mehrjardi et al., 2012, Hegde and Sitharam, 2015b), yet there is a lack of investigation into the protection of pipes buried in trenches (that are then trafficked repeatedly) by the combined use both of EPS block and geocell reinforcement. It is the aim of this paper to address this combination under repeated loading as a potential means of providing pipe protection and a trafficable ground surface over the pipe where positive arching is operative.

2. Goals

Many buried pipes in shallow or deep trench backfill are made of flexible material, such as uPVC (unplasticized polyvinyl chloride) and HDPE (high density polyethylene). Thus, to increase the required serviceability period and to protect the pipe from the applied stress induced by static and repeated loading at the ground surface, special attention must be given to the backfill arrangements. The overall goal of the current study was to investigate the beneficial, simultaneous, use of EPS geofoam block and geocell reinforcement in backfill over pipes subjected to simulated repeated loading of heavy traffic by full scale modelling. It was expected that the EPS geofoam block, together with the geocell reinforcement, would reduce pipe deformation and transferred pressure to the buried pipe while limiting the trench settlement to an acceptable value. Thus a total of 14 independent tests (plus 17 repeated tests) were performed on a buried pipe in unreinforced and geocell-reinforced soil, with and without EPS geofoam blocks.

123 It should be noted that in the testing program, only one type of pipe, one type of geocell, one type of soil
124 and one density of EPS block were used. The results should, therefore, have direct applicability, qualitatively,
125 to the applications envisaged and could have wider application for buried pipe installation, but will need
126 adjusting for different soil properties, different density of EPS geofoam block and different geosynthetic
127 properties in such cases.

128 **3. Test material**

129 *3.1. Soils*

130 In order to simulate likely usage conditions, yet not to introduce too many variables, a granular soil was
131 used around the two sides of the pipe and to cover the crown. It was also used to cover the EPS block and to
132 fill the geocell pockets (in geocell-reinforced installations), as shown in Fig. 2. The soil has a maximum grain
133 size and mean grain size of 20 mm and 4.3 mm, respectively and a specific gravity of 2.66 (G_s=2.66).
134 According to the Unified Soil Classification System (ASTM D 2487-11), this soil is classified as well-graded
135 sand with letter symbol "SW" which satisfies the grain size limits for pipe backfill materials according to
136 ASTM D 2321-08. Based on the modified proctor compaction, following ASTM D 1557-12, the maximum
137 dry unit weight and the optimum moisture content of this soil were determined as about 20.42 kN/m^3 and
138 5.1%, respectively. The angle of internal friction (φ) of the soil, obtained by consolidated undrained triaxial
139 compression tests of specimens at a wet unit weight of 19.72 kN/m^3 and a moisture content of 5%
140 (corresponding to 92% of maximum dry unit weight, similar to the compacted unit weight of soil layers in
141 backfill) was 40.5°. To simulate the natural ground that would provide the bedding and the two vertical sides
142 of the trench, a soil with grain sizes between 0.08 and 20 mm and with medium cohesion was used.
143 According to the Unified Soil Classification System (ASTM D 2487-11), this soil is classified as well-graded
144 sand with clay (SW-SC).

145 *3.2. Geocell reinforcement*

146 The geocell used is a particular 3D geosynthetic formed from strips of non-woven polymeric geotextile
147 thermo-welded into a form of non-perforated cellular and honeycomb-like system. Table 1 tabulates the
148 engineering properties of this geotextile to form the geocell, as listed by the manufacturer. In all geocell-
149 reinforced tests, the geocell layer was used in two pocket sizes of 55×55 mm^2 or 110×110 mm^2 and one
150 height of 100 mm. When spread out, it occupied an area of 1250×1250 mm^2 in plane (5 times the loading
151 plate in each direction), centred on the axis of loading. An isometric view of the geocell spread below the soil

surface at optimum depth is shown in Fig. 3. According to the manufacturer (Treff, 2011), the strength and stiffness of the geocell joint is higher than or similar to that of the geocell wall material (i.e. geotextile).

3.3. Pipe

With regard to technology development and the increasing use of polyethylene pipes in urban drainage and sewerage system, polyethylene pipes complying with BSI 4660 (2000) for underground services were used. Initially, several pipes obtained from different manufacturers were subjected to a variety of test evaluations so as to verify the suitability for the testing programme described herein. On this basis, a high density polyethylene pipe (HDPE 100), designed to withstand a pressure of 4 bar, having an outer diameter (D) of 250 mm, a wall thickness (t) of 4 mm and, thus, a Standard Dimension Ratio (SDR) = D/t =40 was selected. Based on the manufacturer (Gostaresh Co.), this pipe has an elastic modulus of 1000 MPa, a Poisson's ratio of 0.3 and a weight per unit length of 4.83 kg/m. A pipe length of 1740mm, approximately equal to the length of the trench in the full scale model test (see Section 4.1) was chosen.

3.4. EPS geofoam block

Expanded Polystyrene (EPS), commonly called “geofoam”, is formed into compressible low-density cellular plastic blocks. In the current study, EPS geofoam blocks with different thicknesses, different widths (as a ratio of pipe diameter, D) and with density of 38 kg/m^3 were evaluated by the testing program. Unconfined uniaxial compressive testing (ASTM D 1621-00) was performed on 200 mm cubic specimens of EPS. The stress-strain response, plotted as Fig. 4, contains four parts: an initial linear response, yield, linear work hardening and, finally, non-linear work hardening – a similar response to previous studies (e.g. Stark et al., 2004). The elastic limit and compressive strength of EPS geofoam are defined as the stress at 1% and 10% strain, respectively (Horvath, 1994). Using this definition, the elastic limit, compressive strength and elastic modulus of EPS material block are 23.88 kPa, 207.27 kPa and 2.39 MPa, respectively. It should be noted that lower density EPS blocks (e.g., lower than 20-25 kg/cm^3) are much more compressible than higher density ones, since both elastic modulus and compressive strength reduce with decrease in EPS density (Horvath, 1996). Because limiting the trench settlement to an acceptable value is one of the aims of this study, thus the combination of geocell reinforcement with higher density EPS geofoam blocks is better than using lower density EPS blocks to limit settlement of the backfill under heavy repeated loading. By considering the quality and durability of the EPS material, the maximum available EPS density of 38 kg/m^3 was selected.

4. Model Test

A full scale model test was used to provide realistic test conditions. The test equipment comprises a model test trench, a loading system and a data measurement system, shown, schematically, in Fig. 5.

4.1. Test trench

The full scale model of the test trench containing the pipe, geocell layer and EPS block was prepared in a test pit with plan dimensions of 2200 mm × 2200 mm and depth of 1000 mm. The test trench was constructed 750 mm wide (X direction) and 750 mm deep (Y direction), as shown in Fig. 5, and 1750 mm long. The trench width was selected to meet the recommendations of BSI (1980), ASTM D2321-08 and AASHTO (2010). The BSI (1980) and ASTM D2321-08 recommend the minimum trench width as D+300 mm and 1.25D+300 mm (where D is the pipe diameter in mm), respectively. According to AASHTO (2010), the minimum width of the trench should be the greater of 1.5D+305 mm and D+406 mm. The maximum buried depth of the pipe was selected as two times the pipe's diameter (2D=500 mm), as proposed by Moghaddas Tafreshi and Tavakoli Mehrjardi (2008), being an optimized value of burial depth for a pipe embedded in geogrid-reinforced soil.

4.2. Loading System and simulated traffic load

The load system includes a loading frame, a hydraulic cylinder and a controlling unit. The loading frame consists of two heavy steel columns and a horizontal strong reaction beam spanning the width of the test pit, which supports the hydraulic actuator. The hydraulic cylinder and controlling unit may produce monotonic or repeated loads with the capability of applying a stepwise controlled load to a maximum capacity of 100 kN. In order to simulate the loads imposed by traffic, loading, unloading and reloading were imposed through a circular plate located at the centre of the trench surface. In all tests, 150 cycles of repeated loading with amplitude of 800 kPa and frequency of 0.33 Hz were applied to the loading plate. The diameter of the loading plate (250 mm) and the maximum applied pressure of 800 kPa were chosen to replicate that of a heavy vehicle half-axle (40 kN) as used on a common heavy trailer (mean tyre pressure 792 kPa) as recommended by Brito et al. (2009).

4.3. Data measurement system

The data measurement system was developed to read and record the applied repeated load, loading plate settlement, pipe deformation and soil pressure automatically. An S-shaped load cell, with an accuracy of ±0.01% and a full-scale capacity of 100 kN, was placed between the hydraulic jack and loading plate to

precisely measure the applied repeated load. To measure the average settlement of the loading plate during loading, unloading and reloading, two linear variable differential transducers (*LVDTs*) with an accuracy of 0.01% of full range (100 mm) were attached to opposite edges of the loading plate.

To measure the pipe deformation during the test, six LVDTs with the accuracy of 0.01% of full range (75 mm) were installed inside the pipe. Two steel U channel profiles were placed inside the pipe to make a solid base on which to fix the LVDTs (by magnet base/rod) that measured horizontal (D_h) and vertical (D_v) deflections at the different points of the pipe (Fig. 6a-b). The first steel U channel was rested inside the pipe to measure the vertical (D_v) deflections. It was only connected via a flexible plastic screw so as to prevent its horizontal displacement but to allow it to record the horizontal (D_h) deflection while minimizing its influence on pipe deformation. Although, this might influence the horizontal (D_h) deflection, it seems should have the same effect in all tests. Five LVDTs were installed to measure the vertical deflection of the pipe crown (D_v) in the middle of the pipe length and along the pipe's axis at distances of 150, 300, 450 and 600 mm from the mid-point of the pipe's length. In some tests, one additional LVDT was installed to measure the horizontal deflection of the pipe at the mid-point of the pipe's length. Fig. 6a-b provides a photograph and a schematic of the LVDTs inside the pipe in the middle and along the pipe's axis, defining the horizontal (D_h) and vertical (D_v) pipe deflection meanings.

The soil pressure around the pipe was monitored and measured by two soil pressure cells (abbreviated to SPC.C and SPC.S) with a diameter of 50 mm and an accuracy of 0.01% of their full range of 1 MPa. Similar soil pressure cell with diameter of 50 mm was used by Palmeira and Andrade (2010) to investigate the behaviour of buried pipes in geosynthetic reinforced backfill. Pressure cell "C" (SPC.C) was installed on the crown of pipe to measure the vertical soil pressure, while pressure cell "S", (SPC.S) was installed at the springline of the pipe to measure the lateral soil pressure as shown in Fig. 5 and Fig. 6c. To calibrate the pressure cells, a 300 mm-diameter and 200 mm-high cylindrical container made of very soft textile was filled with soft and fine soil and the cell placed in the middle. Although, the use of soft soil around the cell's diaphragm instead of the actual granular backfill soil might have influenced the soil pressure measurements, to prevent damage of the diaphragm of the soil pressure cell caused by granular backfill soil with maximum grain size of 20 mm, the manufacturer recommends the use of soft soil around the pressure cell. Thereafter by placing the container in a compression machine, the cells were calibrated for different levels of applied pressure. Ideally, cell diameter should be many times the maximum particle size of the soil (Weiler and Kulhawy, 1982, suggest 10 times, other authors as much as 50 times!) – an impractical requirement for these

tests. To overcome this difficulty, following the advice of Palmeira and Andrade (2010), sand-filled bags were used to spread any loads, coming from coarse particle asperities, to the cell diaphragm.

4.4. Test preparation and procedure

In order to compact the backfill layers over the pipe (Fig. 5), a walk-behind vibrating plate compactor, 450 mm in width, was used. In all the tests, the unreinforced soil layers at an optimum moisture content of 5% and wet unit weight of 19.72 kN/m^3 were prepared and compacted at thickness of 50 and 75 mm, respectively by one and two passes of compactor (see Table 2), depending on the thickness of EPS block. To achieve the required density of the soil that filled the pockets of the geocell layer, it was compacted with four passes of the compactor, irrespective of geocell pocket size (see Table 2). Thus the compaction energy, and consequently the compactive effort, was kept the same for all passes of the compactor. The depth of influence of the compactor is reported by the manufacturer to be between 50-100 mm, so additional compaction of the bottom layers due to compaction of the top layer will be significant impact and could be ignored. The soil mass around both sides of the pipe was carefully compacted by dropping a tamper with weight of 5 kg on a rigid steel plate with dimension of 240×240 mm from a height of 300 mm, three times, on the soil surface at two levels of horizontal pipe diameter and pipe crown. It provided a wet unit weight of soil approximately 17 kN/m^3 (see Table 2). Dropping the tamper more than three times caused no significant increase in soil unit weight.

To have a better assessment of the backfill compaction, in some installations and after backfill placement, the unit weight of unreinforced layers and the soil inside the pockets of geocell layer were measured according to ASTM D 1556-07 (Table 2). The measurements showed that the unit weight of the unreinforced layers is greater than that inside the geocell pockets due to compaction difficulty of soil inside the geocell pockets. This is a problem observed by previous researchers (Thakur et al., 2012; Tavakoli Mehrjardi et al, 2013; Moghaddas Tafreshi et al., 2013). The densities measured in several compacted layers in each series of tests, revealed a close match between the unit weight values obtained from cone tests and the required unit weight values with maximum differences in results of ≈2-3%. This difference seems to be small for geotechnical applications. Table 2 shows the average measured dry densities of unreinforced soil and the soil filled in the geocell pockets after compaction of each layers. As the backfill was placed and compacted, the two pressure cells on the crown and at the springline of the pipe were installed.

When the backfill was complete, the loading plate was exactly set at the centre of backfill and two LVDTs were installed to record the settlement at the loaded surface. Fig. 7 illustrates a photograph of pipe and test installation prior to loading.

5. Test program

The test configurations and their geometry for buried pipes in both unreinforced and geocell-reinforced backfill, with and without EPS blocks, as considered in these investigations, is shown in Fig. 8. In addition, Table 3 gives details of the test series performed in this study. In the case of the backfill without any EPS block, two series of tests (Test Series 1 and 2 (Fig. 8a-b)) were conducted under unreinforced and geocell-reinforced conditions. The width of the geocell layer (b) and the depth to the top of the geocell layer below the footing (u) were held constant (for Test Series 2 and 4) respectively at 5 and 0.2 times the loading plate diameter (optimum values as determined by Moghaddas Tafreshi et al, 2013; 2014). The thickness of the geocell layer inside the backfill was held constant in all the tests at 100 mm. The performance of the EPS blocks on the behaviour of pipe, buried under both unreinforced and geocell-reinforced backfills, is the subject of Test Series 3 and 4 (Fig. 8c-d). In these two Test Series, the effect of EPS block thickness (h_e) and EPS block width (w) as two dimensionless parameters of h_e/D and w/D were investigated.

Several of the tests listed in Table 4 were repeated, at least twice. By this means the apparatus, data collection accuracy/consistency, system repeatability and reliability of the results could be assessed. The findings reveal a high similarity between results of the replicate tests, with a difference between results always less than 5% - an acceptably small, and negligible, difference in geotechnical testing. It was concluded that the combination of equipment and test procedure permits repeatable results to be obtained.

6. Results and discussion

In this section, the test results obtained from the full scale model are presented with a discussion highlighting the effects of the various parameters. The presentation of all the result figures would have made the paper lengthy, so only a selection is presented. Note that the deflections of the pipe are presented as vertical (ΔD_v) and horizontal (ΔD_h) diameter changes as a proportion of the original pipe diameter, D (i.e. $\Delta D_{v=} D_v/D$ and $\Delta D_{h=} D_h/D$), expressed as a percentage.

6.1. The typical trends of test results

Fig. 9a-b shows the typical trends of the vertical pipe crown displacement (ΔD_v) and the soil surface settlement (SSS) with the number of load cycles during the repeated loading. As seen in this figure, the rate of increase in ΔD_v (or SSS) decreases as the number of load cycles increase. It illustrates that, in this

condition of tests and due to 150 load cycles with frequency of 0.33 Hz, the variation of ΔD_v and SSS becomes approximately stable and it can be anticipated to reach a fully stabilized condition with only a few additional cycles of load. This may be attributed to the early process of reorientation of particles in the side fill of the pipe and beneath the loading, causing local side fill stiffening, but which ceases relative rapidly allowing the system to reach elastic stability (Faragher et al., 2000) (i.e. a shakedown condition).

The pressure-SSS or pressure-ΔD_v plots derived from these tests are shown in Fig. 9c-d. Although initial plastic strain occurs, it is clear that for repeated loads on the soil surface, a steady response condition was approximately achieved when the load path formed a closed hysteresis loop, indicating only a small amount of energy lost in the system. The other fact seen in Fig. 9, associated with the general behavior of the buried pipes subjected to repeated loads, is the large proportion of the pipe deformation/soil surface settlement at the end of the first pulse compared with its total pipe deformation/soil surface settlement due to many, later, load cycles. Again, this helps to support the conjecture that the first pulse is largely causing compactive action on, i.e. large plastic strain in, the surrounding soils. In this case, 30 or 27% of the total ΔD_v or SSS, respectively, occurs during the first cycle.

Fig. 10 demonstrates the typical variation of pressure on the pipe crown (as measured by SPC. C), with the number of load cycles and its hysteresis curve, for the same test condition as in Fig. 9. As seen in Fig. 10a, the rate of increase in pressure reduces with increase in the number of load cycles and a stable condition was achieved at only 50 cycles (approx.). Indeed, after only a single cycle of load approximately 70% of the final pressure has been imposed. This observation, alongside the occurrence of a closed hysteresis loop (Fig. 10b) much more rapidly than in Fig. 9c-d, suggests that pipe bedding and side fill compaction is completed easily but that full compaction of the fill above the pipe requires more effort.

6.2. The influence of geocell reinforcement (no EPS block in the backfill)

Fig. 11 compares the response of the buried pipe in the unreinforced and geocell-reinforced systems (Test Series 1 and 2 in Table 3) through 150 cycles of repeated loading. Both Soil Surface Settlement (rut depth on soil surface) and vertical and horizontal pipe diameter changes are smaller when the geocell is in place, evidence of beneficial stiffening and load-spreading abilities of the geocell installation under repeated loading. As seen in Fig. 11a, the soil surface settlement of the reinforced installation, at the last load cycle decreased by 25% to 45%, respectively, for small and large pocket geocell installations (compared to the unreinforced installation).

Fig. 11b plots the changes in vertical and horizontal diameter of pipe (ΔD_v and ΔD_h) against the load cycles and illustrates a decrease in the vertical diameter of the pipe (i.e., negative ΔD_v) and an increase in horizontal diameter of the pipe (i.e., positive ΔD_h) as the load cycles increase. From Fig. 10b, the values of ΔD_v of the pipe at the end of load cycling for unreinforced and geocell-reinforced tests with small and large geocell pocket sizes were obtained as 8.74%, 7.12% and 6.35%, respectively. Also, the corresponding values for ΔD_h are 7.12%, 6.73 and 6.12%. These values indicate an improvement in ΔD_v by about 27.4% and ΔD_h by about 14.04% due to the large pocket geocell reinforcement. Thus, the competent performance of the geocell reinforced system in reducing the pipe deformation is evidenced as well as that in decreasing the soil surface settlement.

To gain a better assessment of the pipe deformation, the variation of the pipe's vertical deflection at its crown, along the pipe's longitudinal axis (at distances of zero, 150, 300, 450 and 600 mm from the middle of pipe's length) at the end of load cycling is presented in Fig. 11c. The zero-value on the horizontal axis of this figure indicates the point on the crown beneath the center of the loading surface and the axis indicates the distance along the pipe's axis from zero point. As expected, the deflection of the pipe's crown decreases away from the centre of loading for both unreinforced and reinforced systems. From Fig. 11c, for the buried pipe in unreinforced backfill, the vertical deflection of pipe (ΔD_v) at the distances of zero, 150, 300 and 450 mm from the middle of pipe length are about 8.74%, 6.52%, 3.89%, 1.63% and 0.23%. The corresponding values for geocell-reinforced system with small pocket size are about 7.12%, 5.56%, 3.62%, 1.28% and 0.19% and for geocell-reinforced system with large pocket size are about 6.35%, 4.86%, 3.18%, 1.16% and 0.15%. It indicates that using the geocell layer beneath the soil surface, rendered the buried pipe system considerably protected. As can be seen in Fig. 11c, there was a non-linear variation of pipe crown deformation along the pipe's longitudinal axis, and it converges to an insignificant value over 600 mm from the centre of the loaded area. Fig. 11c also implies that the length of pipe is large enough that behaviour at the centre of the pipe's length can be assumed to be unaffected by the two pipe ends.

Fig. 11d demonstrates the variation of the measured pressure on the crown (SPC. C) and at the springline of the pipe (SPC. S) with load cycles, for both unreinforced and geocell-reinforced systems. The readings show that, in the last cycle of loading, the transferred stress on the crown (measured at SPC 'C') and at the springline of the pipe (measured at SPC. 'S') are about 75% and 92% of the values in the unreinforced installation, respectively, for large pocket size geocell and 86% and 95% for small pocket size geocell. These ratios imply that lateral pressure at the springline of the pipe (SPC. S) is not remarkably affected by the

358 geocell reinforcement (the factor is about 0.92-0.95). However, Fig. 11d indicates that the observed reduction
359 in pipe deflection in Fig. 11b could be attributed to a lower transferred pressure on the pipe crown. Thus,
360 horizontally, a much stiffer arrangement has resulted. It is assumed that this reflects improved load spreading
361 achieved by the geocell which is spreading load away from the crown (with a matching reduction in
362 deflection there) and spreading it somewhat to the pipe margins. There, it is assumed, passive, horizontal
363 earth pressure is now developed by smaller pipe deflections than before, due to the better compacted soil that
364 has resulted from the increase in vertical load that has been spread to it. The improvement in the behaviour of
365 pipes due to provision of reinforcement is in the line with the finding of Moghaddas Tafreshi and Khalaj
366 (2008) and Tavakoli Mehrjardi et al. (2012), Hegde and Sitharam (2015b).

367 Fig. 11 shows that the 110×110×100 mm geocell installation delivers greater benefit, for all tests, than
368 does the 55×55×50 mm geocell arrangement. It proved impossible to achieve as great a density of pocket
369 infill in the small pockets as in the large (see Table 2) - despite preparing and compacting the infill soil in the
370 same manner. Probably, the greater number of vertical pocket sides found in the smaller geocell than in its
371 larger 'brother' offered a greater hindrance to compaction. A further factor may be the greater number of
372 (inevitable) break-ups between otherwise interlocked soil particles. These reductions in density and in stone-
373 stone interaction are unavoidable, as noted by previous authors (Thom, 2008; Tavakoli Mehrjardi et al.,
374 2013). Thus, for the later tests (Series 4 = geocell-reinforceds with EPS blocks), the larger geocell
375 (110×110×100 mm pockets) was used.

376 On the basis of the foregoing, the following reasons are suggested for the improved performance when
377 geocell is present:

378 • The honeycomb structure of a geocell layer imposes a hoop stress on soil in a pocket, preventing it
379 from being sheared away from the load. Hence, overall, there is an effective increase in shear
380 strength of the composite system with a consequential reduction in soil surface settlement (Tavakoli
381 Mehrjardi et al., 2012; Thakur et al., 2012; Moghaddas Tafreshi et al., 2014).

382 • The soil in the geocell is, relative to the unreinforced soil, stiff in bending due to its increased
383 confinement. Therefore, it acts to redistributes stress more widely. In turn this reduces the vertical
384 stress applied to the underlying soil in the central area so that the stress applied to the pipe is also
385 reduced. In its turn this leads to a reduction in pipe deformation compared to the unreinforced
386 situation.

6.3. The influence of EPS block

The effect of EPS block on the trench settlement and behaviour of the buried pipe in the unreinforced and geocell-reinforced systems was investigated in Test Series 3-4 (Table 3). In these tests the effect of width and thickness of EPS block were examined.

6.3.1. The influence of EPS block width in unreinforced and geocell-reinforcement installations

To investigate the influence of EPS block width on the pipe behaviour in unreinforced and geocell reinforced backfills, the first row of Test Series 3 and 4 were performed. For unreinforced installations, four widths of EPS (D, 1.5D, 2D and 2.5D (Fig.12)) and for geocell-reinforced installation three widths (D, 1.5D and 2.5D (Fig. 13)) were examined for a fixed EPS block thickness of 0.6D (h_e=0.6D). The results of all the unreinforced tests (i.e. the backfill was installed with EPS block but the geocell layer was not used at the top of the backfill) and geocell-reinforced tests (i.e. the backfill was installed with EPS block) are presented in Fig. 12 and Fig. 13, respectively, showing soil surface settlement (SSS), vertical diameter change (ΔD_v) and pressure variation under 150 repetitions of loading.

Figs. 12a-b and 13a-b reveal that for both unreinforced and geocell-reinforced installations, with increase in the number of load cycles, the amount of soil surface settlement (SSS) and vertical diameter change (ΔD_v) of the pipe steadily increase, with a large proportion of the total SSS and ΔD_v (as recorded after all cycles (N=150)) occurring during the first cycle of loading (N=1). For example, the ratio of SSS during the first load cycle (N=1) to that accumulated by the last cycle (N=150) changes from 27% to 36%, regardless of unreinforced and geocell reinforced installations. Also, the corresponding values for ΔD_v are from 35% to 46%.

Figs. 12a and 13a also illustrate that, with increase in the width of EPS block, the amount of SSS increases. As seen in Fig.12a, an EPS block in the unreinforced installation (without any geocell-reinforcement) does make the SSS behaviour worse. e.g. for the EPS block with widths of 2D and 2.5D, unstable conditions with large settlement of 88.8 and 88 mm occur at load cycles 5 and 75, respectively, (long before reaching load cycle of 150). For the EPS block with widths of D and 1.5D, excessive settlement could be expected with further loading cycles unless soil permanently bridges over the blocks.

According to the results presented in Section 6.2 and Fig. 11, it is expected that a geocell installation over the EPS block could help to attenuate the soil settlement and rectify the negative aspects of an EPS block on soil surface settlement. As shown in Fig.13a, using the geocell layer leads to stabilizing settlement behaviour under repeated loading, irrespective of the EPS block width. Generally, from Fig.12a and 13a the negative

effect of EPS block on soil surface settlement for unreinforced and reinforced backfill is evident although its extent is curtailed by the geocell.

In contrast to the undesirable effect of EPS block on the soil surface settlement (Figs. 12a and 13a), Figs. 12b-d and 13b-d illustrate the beneficial influence of EPS block inclusion on reduction of vertical diameter change (ΔD_v) of the pipe at the center and also along the pipe's longitudinal axis, plus the soil pressure around the pipe when the backfill was installed with an EPS block, whether geocell-reinforced or not.

Figs. 12b-c and 13b-c show that the best performance in reducing the vertical deformation of the pipe along the longitudinal axis, belongs to the installation of EPS block with a width of 1.5D over the pipe, which had a value of ΔD_v at the end of load cycle and in the middle of pipe, in unreinforced and geocell-reinforced installations, respectively 5.25% and 3.98%. It is noticeable that, corresponding ΔD_v values for the unreinforced and geocell-reinforced installations with no EPS block, were respectively 8.74% and 6.34%. Likewise, Figs. 12c and 13c depict that the pipe deformation on the pipe crown, along the pipe's longitudinal axis, declines non-linearly to an insignificant value.

Comparing the results in Figs. 12d and 13d show that the geocell-reinforced installation containing EPS block with a width of 1.5D delivers the best performance in soil pressure reduction around the pipe, as its value at the end of load cycle is obtained at about 92.2 kPa and 45.4 kPa, respectively at the crown (SPC. C) and at the springline (SPC. S).

In order to have a clear and direct investigation of the influence of EPS block on the behaviour of unreinforced and geocell reinforcement systems, the variation of soil surface settlement (SSS), vertical diameter change (ΔD_v) of the pipe and pressure acting on the crown of pipe with EPS block width (w/D) at the last load cycle are shown in Fig. 14.

For unreinforced and geocell-reinforced backfill, the soil surface settlement (SSS) value increases as the width of EPS block is increasing (see Fig. 14a). It could be attributed to the compressibility of the EPS block and also to an increase in its flexibility in the direction of the horizontal diameter of pipe with increase in the width of EPS block; as a result, more bending and deflection in the middle of block and more settlement beneath the loading surface will be experienced.

The variation of the vertical diameter change (ΔD_v) of the pipe and the pressure acting on the crown of pipe with w/D ratio are the subject of Fig. 14b-c, respectively. As seen in these parts of the figure, when an EPS block is installed above the pipe, the value of ΔD_v and the pressure over the pipe decreases, regardless of EPS width, for both unreinforced and reinforced systems when compared with no-EPS block installations.

447 This can be attributed to placing EPS block as an additional compressible inclusion above the pipe that can
448 induce more settlement in the soil-EPS prism above the pipe compared to the soils adjacent to the soil prism.
449 Therefore, the more upward shear strength on the two side of soil prism surface would be mobilized which
450 can reduce the pressure on the pipe's crown, consequently the value of ΔD_v decreases (see Fig. 1).

451 From this figure it has also been found that with an increase in w/D ratio to about 1.5, the value of ΔD_v
452 and the pressure acting on the pipe crown decrease down to the minimum value, after which, with increase in
453 w/D ratio, their values increase, irrespective of whether unreinforced or geocell-reinforced. The value of ΔD_v
454 in unreinforced and geocell-reinforced installations that included an EPS block was 5.25% and 3.98%,
455 respectively, at the end of load cycling. These values are respectively about 0.60 and 0.46 times the value of
456 fully unreinforced backfill, which is 8.74%. In a similar way, the measured pressure acting on the pipe crown
457 at the end of load cycling was about 113 kPa and 92 kPa, respectively for the unreinforced and geocell-
458 reinforced installations that included an EPS block, and these values are respectively about 0.47 and 0.38
459 times the value when fully unreinforced (≈243 kPa). Kim et al. (2010) in their studies on buried pipes under
460 EPS geofoam inclusions (with no geosynthetics reinforcement) under three applied static surcharges, reported
461 an optimum value of 1.5D for width of EPS block that gives a 73% reduction in vertical pressure acting on
462 the pipe. The greater reduction in vertical pressure reported by Kim et al. (2010), compared to that observed
463 in current study, might be attributed to the loading type (static versus repeated loadings), thickness and
464 density of EPS block.

465 As seen in Fig. 14, an EPS width of 1.5D gives the minimum value of ΔD_v and pressure on pipe, but there
466 was no significant difference in ΔD_v and soil pressure when an EPS width of 1D was used (the difference is
467 less than 2.5% in value of ΔD_v and less than 9% in value of soil pressure for reinforced installation). The
468 small reduction in ΔD_v and soil pressure when the EPS width changes from 1 to 1.5 times the pipe diameter
469 suggests that an optimal width of an EPS is approximately 1 to 1.5 times the pipe diameter among the other
470 EPS block widths. As shown in Fig. 14, with the increase in w/D beyond the optimal width of EPS (i.e. 1.5
471 times the pipe diameter), not only is no further improvement generated, but it also counteracts the beneficial
472 effect of an EPS block, as negative influence of pipe behaviour would be expected with increase in the width
473 of an EPS block further than 2.5 times the pipe diameter. This could be attributed to diminishing the arching
474 effect over the pipe due to the use of a wider EPS width which extends the soil prism over the pipe (Kim et
475 al. 2010; Witthoeft and Kim, 2015).

6.3.2. The influence of EPS block thickness in unreinforced and geocell-reinforcement installations

To investigate the influence of EPS block thickness on the pipe behaviour, Test Series 3 and 4 (second row of each series in Table 3) with a fixed ratio of EPS block width to pipe diameter of 1.5 (w=1.5D as optimum value) were performed. For unreinforced installations three thicknesses of 0.1D, 0.3D and 0.6D (Fig.15) and for geocell-reinforced installations three thicknesses of 0.3D, 0.4D and 0.6D (Fig. 16) were examined. The results of all the unreinforced and geocell-reinforced tests with and without EPS block, for 150 cycles of loading, are shown in Figs. 15 and 16, respectively.

Figs. 15a and 16a illustrate the variations of soil surface settlement with number of load cycles for unreinforced and geocell-reinforced installations with and without EPS block. As seen in these figures, for all tests with an EPS block above the pipe, the SSS value is larger than when there is no EPS block. They also indicate that, with increase in the thickness of EPS block, the settlement of the loading surface increases, irrespective of unreinforced and geocell-reinforced installations. This is due to the compressible nature of the EPS inclusions inside the backfill, over the pipe, leading to increased the soil surface settlement. Moreover, referring to Fig. 16a, the geocell effect in decreasing SSS values, when compared with the corresponding no-geocell SSS values in Fig. 15a, is remarkable.

The variation of vertical (ΔD_v) and horizontal (ΔD_h) diameter changes of the pipe, vertical diameter change (ΔD_v) of the pipe along the pipe's longitudinal axis, and pressure around the pipe with number of load cycles for unreinforced and geocell-reinforced installations, are respectively the subjects of Figs. 15b-d and 16b-d. From these figures, reduction in pipe deformation and pressure around the pipe due to the positive influence of EPS block inclusion can be observed for both unreinforced and geocell-reinforced systems. As seen, pipe deformation and vertical pressure on the pipe reduce with an increase in EPS block thickness. This is because, when the soil prism over the pipe contains thicker EPS, then the EPS compression causes more settlement (see Figs. 15a and 16a) relative to the two adjacent soil prisms, which results in a positive arching effect (see Fig. 1). In contrast, a thin EPS layer (e.g. here h_e=0.1D) is not large enough to generate sufficient differential deformation in the soil prisms over the pipe – and so the arching support is not developed. Similar results under applied static load on trench surface have been reported by Beju and Mandal (2017) on vertical pressure reduction on a buried pipe with increase in EPS geofoam thickness. However, as before, the internal benefits of reduced stress on, and deformation of, the pipe are bought at the cost of increases in the settlement of the loading surface settlement (Figs. 15a and 16a).

In addition, an interesting observation that can be made from Figs. 15d and 16d (also observations in Figs. 10a, 11d, 12d and 13d) is that the pressure around the pipe reaches a maximum value during the first load cycles but then tends to decrease to a somewhat smaller value. The reason for this cannot be determined with certainty, but is likely due to rearrangement of the bedding around the pipe, perhaps as the polymeric pipe slowly creeps under load.

To gain a better understanding of the effect of EPS block thickness on the soil surface settlement (SSS) of unreinforced and geocell-reinforced systems, the increase of SSS with EPS block thickness (h_e/D), at the last load cycle, are shown in Fig. 17a. As can be seen, an increase in the thickness of EPS block in the range of 0-0.3D, results in a slow increase in the SSS value, while increasing the EPS block thickness beyond 0.3D results in the rate of enhancement increasing considerably, for both unreinforced and reinforced installations. For example, in unreinforced installation, the SSS value at load cycle 150 are about 52.4, 55.2, 57.2 and 85.6 mm respectively for EPS thicknesses of 0, 0.1D, 0.3D and 0.6D. The SSS value increases about 9.2% when the thinnest EPS block (h_e=0.3D) is inserted, while it increases by some 49.7% when the EPS thickness changes from 0.3D to 0.6D. For geocell-reinforced systems, the rate of increase in SSS value for variation of EPS block thickness between 0.3D and 0.6D is, similarly, substantially greater than when EPS block thickness changes from zero to 0.3D.

Figs. 17b and 17c represent, respectively, the variation of the vertical diameter change (ΔD_v) of the pipe and the pressure acting on the crown of pipe, both with h_e/D ratio, at the last load cycle. As can be seen, the EPS block is able to significantly improve the pipe behaviour, as with increase in EPS thickness, both ΔD_v and pressure on the pipe crown decrease, whether reinforced with geocell or not. This performance improvement seems to be a result of the increase in upward shear strength mobilized on the two side of soil prism surface above the pipe, due to increase in soil surface settlement (Figs. 1 and 17a) which can reduce the pressure on the pipe crown, consequently leading to a decrease in the value of ΔD_v. However, as shown in Fig.17, the rate of decrease in the value of ΔD_v and pressure on pipe when changing in EPS block thickness from zero (no EPS block) to 0.3D, is far greater than when changing from 0.3D to 0.6D, irrespective of reinforcement, suggesting that the soil arching effect is induced even by low thickness of compressible EPS.

7. Discussion of results

EPS Geofoam block has been suggested as compressible inclusion for use over buried pipes by several authors (Vaslestad et al., 1994; Kim et al. 2010; Witthoeft and Kim, 2015; Anil et al., 2015; Beju and Mandal, 2017). The majority of the studies have been only focused on the effect of EPS block geometry on

pressure reduction over pipe. As yet, there is no clear report in the literature regarding the effect of EPS block on pipe deformation and soil loading surface settlement. Yet limiting the soil settlement (rut depth on soil surface) and the pipe deformation must also be considered as essential requirements for a safe and effective backfill trench and buried pipe system. Furthermore, the recommendations of the previous literature are not quantitatively consistent. For example, Vaslestad et al. (1994) recommended using an EPS block with a minimum width larger than 1.5 times the pipe diameter while Kim and Yoo (2005) showed that no significant load reduction was achieved for the EPS panel width of greater than 1.5 times of the pipe diameter.

Table 4 compares the values of soil surface settlement (SSS), vertical diameter change of pipe (ΔD_v) and pressure on the pipe crown for different backfill installations, at the last cycle of loading. For real pipe installation, AASHTO (2010) recommended limiting the vertical diameter change of a pipe (ΔD_v) to 5% as the criteria to avoid snap-through buckling to the pipe. For surface settlement (ruts) AASHTO (1993) recommends a limit of 30-70 mm for unsealed low volume roads. Given that the test results presented here show that the majority of the settlement at the surface occurs in the first 50 cycles or so, this deformation is likely to be caused by construction traffic when an unsealed surface is present. Where a bound surface is to be placed over the top of the trench fill before such settlement has been induced, less rutting is permissible, but the results presented do not give information about the settlement can then be expected. Doubtless the bound material will provide better bridging over the trench than would unbound materials, but the degree of assistance provided and its reliability in the long term would need further study.

For the different test conditions considered here and the summarized results in Table 4, the following discussion could be useful:

(1) For the tests with no EPS block, the benefits of geocell over the unreinforced situation are clear for all measurements, soil surface settlement (SSS), vertical diameter change of pipe (ΔD_v) and pressure on pipe. The geocell reinforcement is able to significantly reduce SSS, ΔD_v and pressure on pipe by about 43%, 27.4% and 24.7%, respectively, compared with unreinforced installations but, even so, the value of ΔD_v is never in the range of allowable recommended value by AASHTO (2010).

(2) Among all the unreinforced installations with EPS block, both the values of ΔD_v and pressure on pipe take their minimum values (5.25% and 113 kPa respectively for ΔD_v and pressure on pipe) for the use of EPS block with thickness of 0.6D (h_e=0.6D) and width of 1.5D (w=1.5D) while the SSS value increases to 85.62 mm which is greater than that obtained for the unreinforced installation with no EPS block. However, it shows that this geometry of EPS block did not satisfy the defined criteria by AASHTO (1993; 2010) for ΔD_v

565 and SSS. Thus, if pipe deformation with no consideration on soil surface settlement (e.g. beneath untrafficked
566 soil) is of primary concern then the use of EPS block with h_e=0.6D and w=1.5D in backfill has the most
567 benefit which protects the pipe from snap-through buckling AASHTO (2010).

568 (3) When geocell reinforcement and EPS are combined, a marked benefit in reduction of both ΔD_v and
569 pressure on pipe are evident, but it results in a larger, soil surface settlement (SSS) compared with the geocell
570 reinforcement-only case. Based on the results in Table 4, using geocell reinforcement and EPS block with
571 h_e=0.6D and w=1.5D could minimize ΔD_v and pressure on pipe at values of 3.98% and 92 kPa, respectively,
572 while SSS values is minimized at 31.53 mm using EPS block with h_e=0.3D and w=1.5D. Also, Table 4
573 shows that the use of EPS block with h_e=0.3D and w=1.5D shows only a little additional enhancement of
574 ΔD_v in comparison with EPS block with h_e=0.6D and w=1.5D while not only does ΔD_v remain less than the
575 5% criteria of AASHTO (2010), but it is also economical to halve the use of EPS – a material more
576 expensive than the soil and geocell reinforcement.

577 Thus, from the results described, using an EPS block with h_e=0.3D and w=1.5D over the pipe in a
578 geocell-reinforced installation, delivered the most acceptable soil surface settlement and pipe deflection
579 design among all the installations. However, of course, an economic evaluation would need to be added to
580 this technical assessment in order to confirm its cost-effectiveness and to arrive at a final decision.

581 **7. Summary and conclusions**

582 The maintenance and the serviceability periods of buried pipes impose major cost to utility companies.
583 For this reason, the long-term functionality and safety of buried pipe systems is a critical requirement when
584 the system is subjected to heavy traffic loading. In this study, a series of full scale tests on buried pipes
585 subjected to simulated heavy traffic loading were conducted to investigate the beneficial, simultaneous, use
586 of EPS geofoam block and geocell reinforcement in backfill over pipes on the reduction of soil surface
587 settlement (rut), pipe deformation and soil pressure acting on the pipe. The parameters studied in the testing
588 program included the pocket size of the geocell reinforcement, the width and thickness of EPS block. Based
589 on the results obtained from the present study, the following conclusions can be derived:

590 (1) The rate of increase in soil surface settlement (SSS), pipe deformation (ΔD_v and ΔD_h) and pressure
591 around the pipe decrease as the number of load cycles increase. A stable condition (for these parameters)
592 could be achieved by installation of the geocell layer and EPS block with appropriate width and thickness.

(2) Large proportions of the total, final, pipe deformation, soil surface settlement and pressure on pipe occurred during the few first load cycles.

(3) The beneficial performance of a geocell mat with large pockets (100mm) on the buried pipe system with and without EPS block was evident. Adding just geocell above the pipe decreased the vertical pipe diameter deflection, soil surface settlement and pressure on pipe crown, respectively, by about 27%, 43% and 25%, but did not deliver a pipe deformation that satisfied the AASHTO (2010) specification.

(4) The use of EPS block over the pipe increased the soil surface settlement, but decreased the pressure transferred onto the pipe and the deformation of pipe for both unreinforced and geocell-reinforced installations.

(5) When adding just EPS block (of thickness 0.6D and width 1.5D) above the pipe, minimum values of ΔD_v = 5.25%, vertical pressure on pipe crown = 113 kPa and soil surface settlement = 85.62 mm were obtained, indicating that neither of the AASHTO (1993 and 2010) criteria have been satisfied.

(6) For the simultaneous installation of EPS geofoam block and geocell reinforcement in backfill, the geocell reinforcement significantly negates the tendency of an EPS block in increasing the soil surface settlement, and also provides more reduction in pipe deformation and pressure acting on pipe.

(7) When adding both geocell and EPS block (of thickness 0.6D and width 1.5D) above the pipe, vertical pipe diameter change and pressure on pipe were 3.98% and 92 kPa, respectively. Also, soil surface settlement was minimized at 31.53 mm by using an EPS block with thickness of 0.3D and width of 1.5D but shows little increase, regarding pipe deformation although the criteria of AASHTO (1993 and 2010) were thereby satisfied.

(8) Overall, for the range of performed tests and to minimize the use of EPS block from an economical point-of-view, this study suggests the use of geocell-reinforced backfill with an EPS block with h_e=0.3D and w=1.5D over the pipe would provide a practical and beneficial solution to protect the pipe and ground surface under heavy traffic loads.

(9) For all installations, a non-linear variation of pipe crown deformation along its longitudinal axis was observed. The pipe deformation converged to an inconsiderable value over 600 mm distance from the centre of loaded area which evidenced, adequately, the length of pipe used in experimental model.

This study can provide insight into the behaviour of the buried pipes protected by geocell reinforcement, in addition to EPS block, subjected to heavy traffic load. Clearly, this is a preliminary study and full application should only be made after considering the limitations and trying a large size model to confirm the

results of this study. The tests results are obtained for only one type of pipe (HDPE pipe with 250 mm external diameter), one type of geocell material, one density of EPS block, one trench width and depth (i.e. one burial depth of pipe) and one type of backfill soil. Hence, it should be noted that the test results applied in this paper might be limited to the size and type of the trench and pipe, soil properties, geocell material and EPS density (which affects its mechanical characteristics such as the strength and elasticity modulus). Hence additional investigations to confirm the results of this study should be considered in future studies. Thus the proposed results should be applied cautiously by considering the above limitations. Also, the economical assessment of EPS blocks, together with geocell layer should be one of the crucial parts of a practical project, but this was not investigated in the current research.

Acknowledgment

The authors thank DuPont de Nemours, Luxembourg, and their UK agents, TDP Limited, for providing the geocell reinforcement used in this test program.

References

American Society for Testing and Materials, 2007. Standard test method for density and unit weight of soil in place by the sand-cone method. ASTM D 1556-07.

American Society for Testing and Materials, 2011. Standard practice for Classification of Soils for Engineering Purposes (Unified Soil Classification System). ASTM D 2487-11.

American Society for Testing and Materials, 2008. Standard practice for underground installation of thermoplastic pipe for sewers and other gravity-flow applications. ASTM D 2321-08.American Society for Testing and Materials, 2012. Standard Test Methods for Laboratory Compaction Characteristics of Soil Using Modified Effort. ASTM D1557-12.

American Society for Testing and Materials, 2000. Standard Test Method for Compressive Properties Of Rigid Cellular Plastics. ASTM D 1621-00.

American Association of State Highway and Transportation Officials. 1993 (AASHTO). Guide for Design of Pavement Structures, AASHTO 1993.

American Association of State Highway and Transportation Officials. 2010 (AASHTO). L. Bridge Construction specifications, AASHTO 2010.

Anil, O.,Tugrul Erdem, R., Kantar, E., (2015). Improving the impact behavior of pipes using geofoam layer for protection. International Journal of Pressure Vessels and Piping. 132-133 (??) 52-64

Barrett, J.C., Valsangkar, A.J. 2009. Effectiveness of connectors in geofoam block construction. Geotextiles and Geomembranes 27(?????) 211-216.

653 Bartlett, S.F., Lingwall, B.N. and Vaslestad, J. 2015. Methods of protecting buried pipelines and culverts in transportation
654 infrastructure using EPS geofoam. Geotextiles and Geomembranes 43 (5): 450-461.
655 Beju, Y. Z., · Mandal, J. N., 2017. Combined use of jute geotextile-EPS geofoam to protect flexible buried pipes:
656 Experimental and numerical studies. Int. J. of Geosynth. and Ground Eng. 3(4): 32.
657 Biabani, M. M., Indraratna, B., Trung Ngo. N., 2016. Modelling of geocell-reinforced subballast subjected to cyclic
658 loading. Geotextiles and Geomembranes 44 (March), 489–503.
659 British Standard Institution (BSI), 1980. Plastics pipework (thermoplastics materials) - Code of practice for the
660 installation of unplasticized PVC pipework for gravity drains and sewers. BS 5955.
661 Brito, L.A.T., Dawson, A.R., Kolisoja, P.J. 2009. Analytical evaluation of unbound granular layers in regard to
662 permanent deformation. In: Proceedings of the 8th International on the Bearing Capacity of Roads, Railways, and
663 Airfields (BCR2A'09), Champaign IL, USA, pp 187-196.
664 Dash, S. K., Rajagopal, K. & Krishnaswamy, N. R. (2007). Behaviour of geocell-reinforced sand beds under strip
665 loading. Canadian Geotechnical Journal, 44, No. 7, 905–916.
666 Dash, S. K., Choudhary, A.W., 2018. Geocell reinforcement for performance improvement of vertical plate anchors in
667 sand. Geotextiles and Geomembranes, 46(2), 214-225.
668 Duskov, M. (1997). Materials research on EPS20 and EPS15 under representative conditions in pavement structures.
669 Geotextiles and Geomembranes, 15(1), 147–181.
670 Farnsworth, C.B., Bartlett, S.F., Negussey, D., Stuedlein, A.W. 2008. Rapid Construction and Settlement Behavior of
671 Embankment Systems on Soft Foundation Soils. Journal of Geotechnical and Geoenvironmental Engineering 134 (3):
672 289-301.
673 Faragher, E., Fleming, P.R., Rogers, C.D.F., 2000. Analysis of repeated-load field testing of buried plastic pipes.
674 Transp.Res. Rec. 1514, Transportation Research Board, Washington, D.C., 271-277.
675 Hatami, K. & Witthoeft, A. F. (2008). A numerical study on the use of geofoam to increase the external stability of
676 reinforced soil walls. Geosynthetics International, 15(6), 452–470.
677 Hegde, A. M., Sitharam, T. G., 2015a. 3-Dimensional numerical modelling of geocell-reinforced sand beds, Geotextiles
678 and Geomembranes, 43(2), 171–81.
679 Hegde, A. M., Sitharam, T.G. 2015b. Experimental and numerical studies on protection of buried pipelines and
680 underground utilities using geocells. Geotextiles and Geomembranes, 43 (5), 372-381.
681 Horvath, J.S. 1994. Expanded Polystyrene (EPS) Geofoam: An Introduction to Material Behavior. Geotextiles and
682 Geomembranes 13 (4): 263-280.
683 Horvath, J.S., 1996. The Compressible-Inclusion Function of EPS Geofoam: An Overview, Proceeding of the
684 International Symposium on EPS Construction Method (EPS Tokyo '96), Tokyo, Japan, October 29–30, EPS
685 Contruction Method Development Organization (EOD), Tokyo, Japan, pp. 71–81.

686 Horvath, J.S. 2010. Emerging Trends in Failures Involving EPS-Block Geofoam Fills. Journal of Performance of
687 Constructed Facilities (ASCE) 24 (4): 365-372.
688 Indraratna, B., Biabani, M.M., Nimbalkar, S., 2015. Behavior of Geocell-Reinforced Subballast Subjected to Cyclic
689 Loading in Plane-Strain Condition. Journal of Geotechnical and Geoenvironmental Engineering. 141(1),
690 Kang, J., Parker, F., Yoo, C.H., 2008a. Soil–structure interaction for deeply buried corrugated steel pipes. Part I:
691 Embankment installation. Engineering Structures. 30 (2), 384–392.
692 Kang, J., Parker, F., Yoo, C.H., 2008b. Soil–structure interaction for deeply buried corrugated steel pipes. Part II:
693 Embankment installation. Engineering Structures. 30(3), 588-594.
694 Keller, G.R. 2016. Application of geosynthetics on low-volume roads. Transportation Geotechnics 8: 119-131.
695 Kim, H., Choi, B. & Kim, J. (2010). Reduction of earth pressure on buried pipes by EPS geofoam inclusions.
696 Geotechnical Testing Journal, 33, No. 4, 1–10.
697 Leshchinsky, B., Ling, H., 2012. Effects of geocell confinement on strength and deformation behavior of gravel. Journal
698 of Geotechnical and Geoenvironmental Engineering, ASCE, 139(2), 340-352.
699 Leshchinsky, B., Ling, H. I., 2013. Numerical modeling of behavior of railway ballasted structure with geocell
700 confinement, Geotextiles and Geomembranes, 36(??), 33–43.
701 Madhavi Latha, G. & Rajagopal, K. (2007). Parametric finite element analyses of geocell supported embankments.
702 Canadian Geotechnical Journal, 44, No. 8, 917–927.
703 Marston, A., 1930, The Theory of External Loads on Closed Conduits in the Light of the Latest Experiments: Bulletin 96,
704 Iowa Engineering Experiment Station, Iowa State College, Ames, IA.
705 Marston, A., Anderson A.O., 1913. The theory of loads on pipes in ditches and tests of cement and clay drain tile and
706 sewer pipes. Bulletin 31. Ames (Iowa): Iowa Engineering Experiment Station.
707 McAfee, R. P. & Valsangkar, A. J. (2004). Geotechnical properties of compressible materials used for induced trench
708 construction. Journal of Testing and Evaluation, 32, No. 2, 143–152.
709 Meguid, M.A., Hussein, M.G., Ahmed, M.R., Omeman, Z., Whalen, J., 2017a. Investigation of soil-geosynthetic-
710 structure interaction associated with induced trench installation. Geotextiles and Geomembranes, (In Press).
711 Meguid, M.A., Ahmed, M.R., Hussein, M., Omeman, Z., 2017b. Earth pressure distribution on a rigid box covered with
712 U-shaped geofoam wrap. International Journal of Geosynthetics and Ground Engineering, 3(2), 1-14.
713 Moghaddas Tafreshi, S.N., Khalaj, O., 2008. Laboratory tests of small-diameter HDPE pipes buried in reinforced sand
714 under repeated-load. Geotextiles and Geomembranes 26(2), 145-163
715 Moghaddas Tafreshi, S.N., Tavakoli Mehrjardi, Gh., 2008. The use of neural network to predict the behaviour of small
716 plastic pipes embedded in reinforced sand and surface settlement under repeated load. Eng. Applications of Artificial
717 Intelligence. 21 (6), 883-894.
718 Moghaddas Tafreshi, S.N., Khalaj, O., Dawson, A.R., 2013. Pilot-scale load tests of a combined multi-layered geocell
719 and rubber-reinforced foundation. Geosynth. Int. 20 (3), 143-161.

720 Moghaddas Tafreshi, S.N., Khalaj, O., Dawson, A.R., 2014. Repeated loading of soil containing granulated rubber and
721 multiple geocell layers. Geotextiles and Geomembranes, 42(1), 25-38.
722 Moghaddas Tafreshi, S.N., Sharifi, P., Dawson, A.R., 2016. Performance of circular footings on sand by use of multiple-
723 geocell or-planar geotextile reinforcing layers. Soils and Foundations 56 (6), 984-997.
724 Newman, M.P., Bartlett, S.F. and Lawton, E.C. 2010. Numerical Modeling of Geofoam Embankments. J. Geotech.
725 Geoenviron. Eng. 136: 290-298.
726 Oliaei, M., Kouzegaran, S., 2017. Efficiency of cellular geosynthetics for foundation reinforcement. Geotextiles and
727 Geomembranes, 45(2), 11-22.
728 Palmeira, E.M., Andrade, H.K.P.A. (2010). Protection of buried pipes against accidental
729 damage using geosynthetics. *Geosynthetics International*, 17(4): 228–241.
730
731 Satyal, S., Leshchinsky, B., Han, J., Neupane. M., 2018. Use of Cellular Confinement for Improved Railway Performance
732 on Soft Subgrades: A Numerical Study. Geotextiles and Geomembranes. 46(2), 190–205.
733 Stark, T.D., Arellano, D., Horvath, J.S., and Leshchinsky, D. 2004. NCHRP Report 529: Guideline and Recommended
734 Standard for Geofoam Applications in Highway Embankments. Transportation Research Board, Washington, D.C.
735 Sun, L., Hopkins, T. C. & Beckham, T. L. (2005). Use of Ultralightweight Geofoam to Reduce Stresses in Highway
736 Culvert Extensions, Publication KTC-05-34/SPR-297-05-1I. Kentucky Transportation Center, University of
737 Kentucky, Frankfort, KN, USA.
738 Sun, L., Hopkins, T. C. & Beckham, T. L. (2009). Reduction of Stresses on Buried Rigid Highway Structures Using the
739 Imperfect Ditch Method and Expanded Polystyrene (Geofoam), Publication KTC-07-14/SPR-228-01-1F. Kentucky
740 Transportation Center, University of Kentucky, Frankfort, KN, USA.
741 Tanyu, B. F., Aydilek, A. H., Lau, A. W., Edil, T. B., Benson, C. H. (2013). Laboratory evaluation of geocell-reinforced
742 gravel subbase over poor subgrades. Geosynthetics International, 20, No. 2, 46–71.
743 Tavakoli Mehrjardi, GH., Moghaddas Tafreshi, S.N., Dawson, A.R., 2012. Combined use of geocell reinforcement and
744 rubber-soil mixtures to improve performance of buried pipes. Geotextiles and Geomembranes, Elsevier, 34 (1), 116-
745 130.
746 Tavakoli Mehrjardi, GH., Moghaddas Tafreshi, S.N., Dawson, A.R., 2013. Pipe response in a geocell-reinforced trench
747 and compaction considerations. Geosynthetics International. 20 (2), 105 –118.
748 Thakur, J. K., Han, J., Pokharel, S. K., Parsons, R. L. (2012). Performance of geocell-reinforced recycled asphalt
749 pavement (RAP) bases over weak subgrade under cyclic plate loading. Geotextiles and Geomembranes, 35, 14–24.
750 Thom, N.H., 2008. Laboratory testing of ground grid reinforced pavements. To Scott Wilson, Nottingham Transportation
751 Engineering Centre, University of Nottingham, UK.
752 Treff, A., 2011. Private Communication with Albert Treff of DuPont de Nemours, Luxembourg.

753 Trung Ngo. N., Indraratna, B., Rujikiatkamjorn, C., Biabani, M. M., 2016. Experimental and Discrete Element Modeling
754 of Geocell-Stabilized Subballast Subjected to Cyclic Loading. Journal of Geotechnical and Geoenvironmental
755 Engineering. 142(4)
756 Vaslestad, J., Johansen, T. H. & Holm, W. (1994). Load Reduction on Buried Rigid Pipes; Load Reduction on Rigid
757 Culverts Beneath High Fills: Long Term Behaviour; Long-Term on EPS Construction Method (EPS Tokyo '96), EPS
758 Construction Method Development Organization, Tokyo, Japan, pp. 31–46.
759 Witthoeft, A., Kim, H. (2015). Numerical investigation of earth pressure reduction on buried pipes using EPS geofoam
760 compressible inclusions. Geosynthetics International, 23(4), 1-14.
761 Zarnani, S. & Bathurst, R. J. (2007). Experimental investigation of EPS geofoam seismic buffers using shaking table
762 tests. Geosynthetics International, 14(3), 165–177.
763 Zou, Y., Small, J.C. and Leo, C.J. 2000. Behavior of EPS Geofoam as Flexible Pavement Subgrade Material in Model
764 Tests. Geosynthetics International. 7 (1): 1-22.
765
766
767
768
769
770
771

Nomenclature

G_s	specific gravity
ϕ	soil angle of internal friction
d	geocell pocket size
h	height of geocell
D	Pipe diameter and diameter of loading surface
b	width of geocell layer
u	embedded depth of geocell layer below the loading surface
h_e	thickness of EPS block
w	width of EPS block
SPC. C	soil pressure cell on pipe crown
SPC. S	soil pressure cell at springline of pipe
$Z=2D$	embedment depth of pipe
D_v	change in vertical diameter
D_h	change in horizontal diameter
$\Delta D_{v=} D_v/D$	vertical diameter change
$\Delta D_{h=} D_h/D$	horizontal diameter change
SSS	soil surface settlement

772
773

774

775

776

777 **List of Tables**

778

779

780

781

782

783

784

785 **List of Figures**

Fig. 10	Typical trend of (a) transferred pressure on pipe with load cycles, (b) hysteresis curve of transferred pressure
Fig. 11	Comparison between geocell-reinforced and unreinforced installations for (a) SSS, (b) ΔD_v and ΔD_h, (c) pipe deformation in longitudinal axis, and (d) Soil pressure on crown and at springline of pipe (SPC. C and SPC. S)
Fig. 12	The effect of EPS block width in unreinforced installation on (a) SSS, (b) ΔD_v, (c) pipe deformation in longitudinal axis, and (d) Soil pressure on crown and at springline of pipe (SPC. C and SPC. S)
Fig. 13	The effect of EPS block width in unreinforced installation on (a) SSS, (b) ΔD_v, (c) pipe deformation in longitudinal axis, and (d) Soil pressure on crown and at springline of pipe (SPC. C and SPC. S)
Fig. 14	Variation of (a) SSS, (b) ΔD_v, and (c) pressure on pipe crown with w/D for unreinforced and geocell-reinforced installations (h_e/D=0.6)
Fig. 15	The effect of EPS block thickness in unreinforced installation on (a) SSS, (b) ΔD_v, and ΔD_h (c) pipe deformation in longitudinal axis, and (d) Soil pressure on crown and at springline of pipe (SPC. C and SPC. S)
Fig. 16	The effect of EPS block thickness in geocell-reinforced installation on (a) SSS, (b) ΔD_v, and ΔD_h (c) pipe deformation in longitudinal axis, and (d) pressure on crown and at springline of pipe (SPC. C and SPC. S)
Fig. 17	Variation of (a) SSS, (b) ΔD_v and (c) pressure on pipe crown with h_e/D for unreinforced and geocell-reinforced installations (w/D=1.5)

786

787

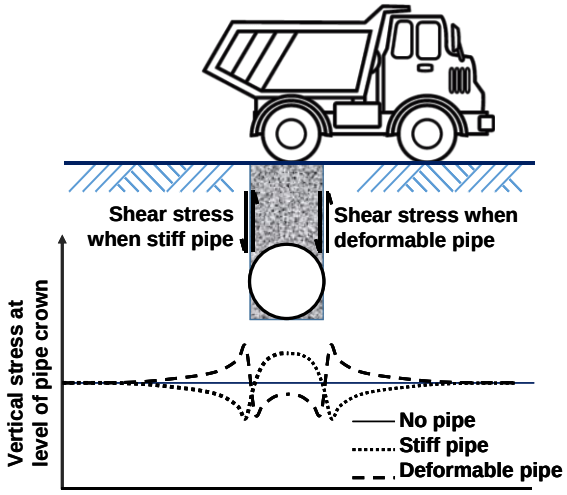

Fig. 1. Conceptual vertical stress distributions at level of pipe crown as a function of deformability of pipe relative to surrounding soil (assuming backfill has same characteristics as surrounding soil)

788

789

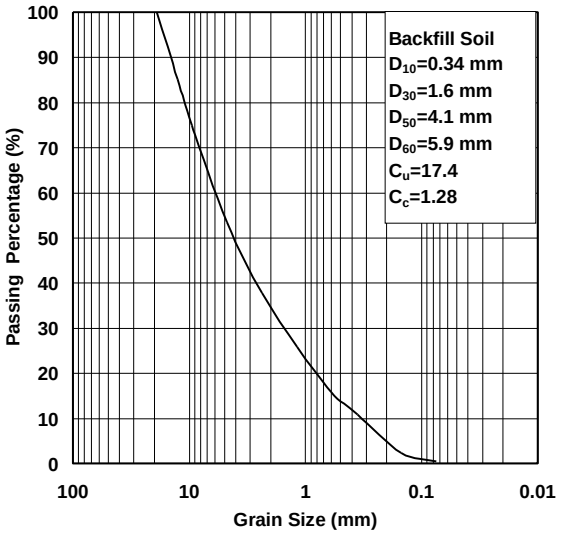

Fig. 2. Grain size distribution curves for backfill soil (ASTM D 2487-11)

790

791

Fig. 3. A view of geocell (TDP Limited) spread over the pipe in the test pit

792

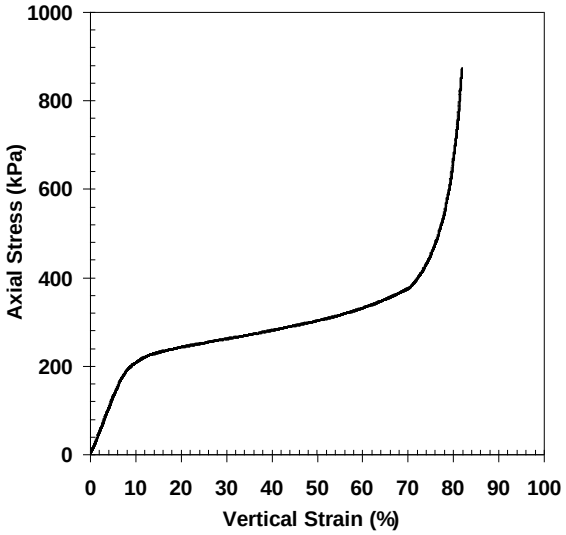

Fig. 4. Unconfined compression stress-strain curves of EPS geofoam block with density of 38 kg/m^3

793

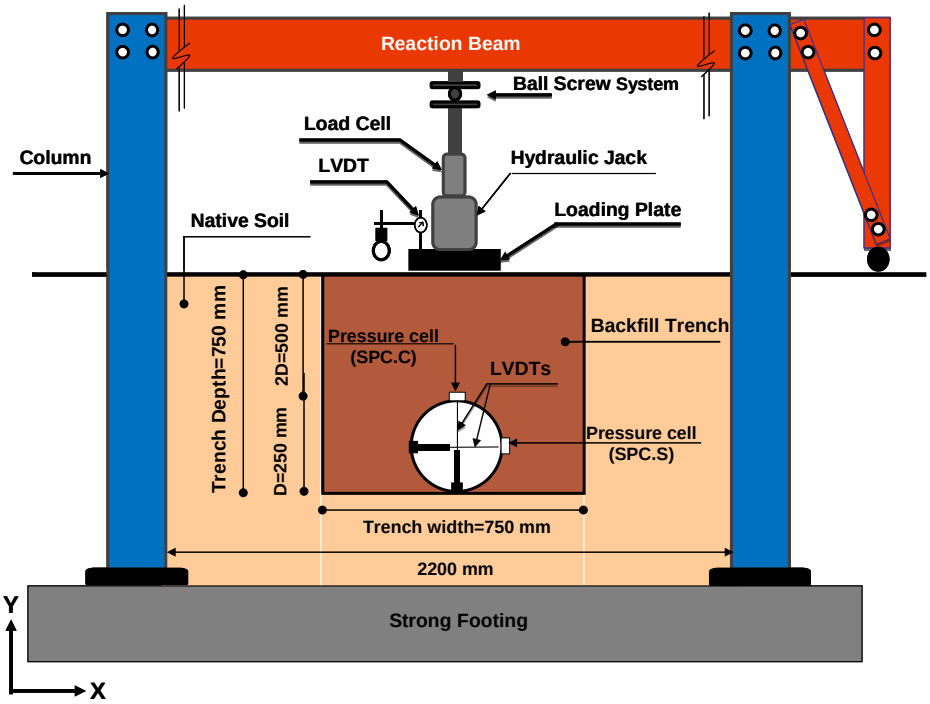

Fig. 5. Schematic view of test setup, instrumentation positions and geometric parameters (unit in mm)

794

795

796

797

798

799

800

801

802

803

804

805

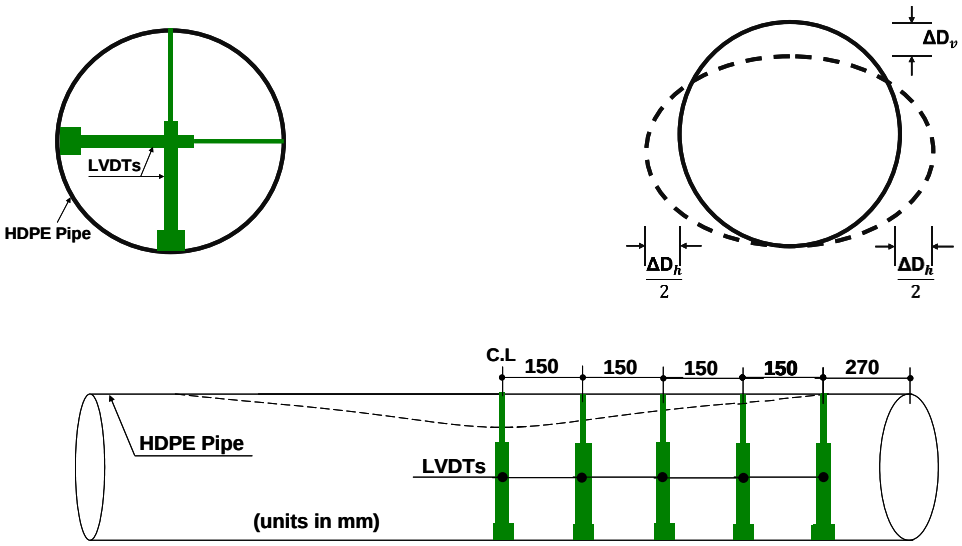

(a)

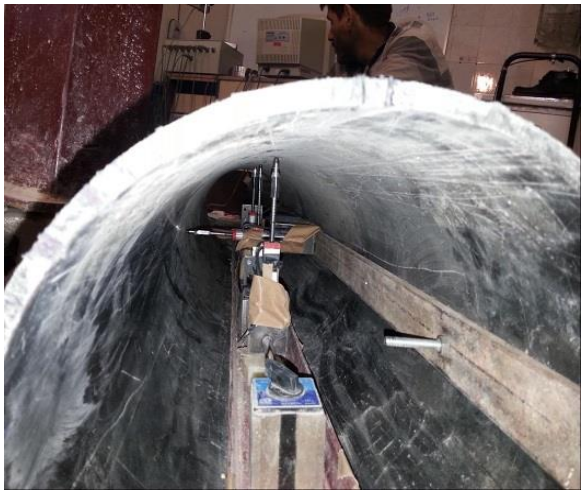

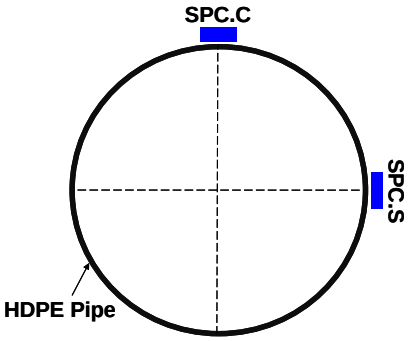

(b) (c)

Fig. 6. Schematic installation of (a) LVDTs inside the pipe and definition of the horizontal (D_h) and vertical (D_v) pipe deflections, (b) Photograph view of LVDTs inside the pipe, (c) Schematic of soil pressure cells on the crown (SPC.C) and at the springline (SPC.S) of the pipe

806

807

(a) (b)

Fig. 7. Photograph of (a) pipe installation in trench (b) test installation prior to loading include reaction beam, load plate, hydraulic jack, load cell and LVDTs

808

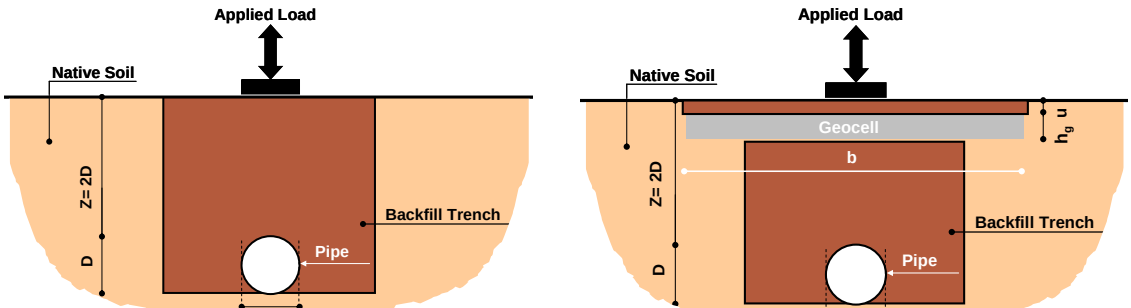

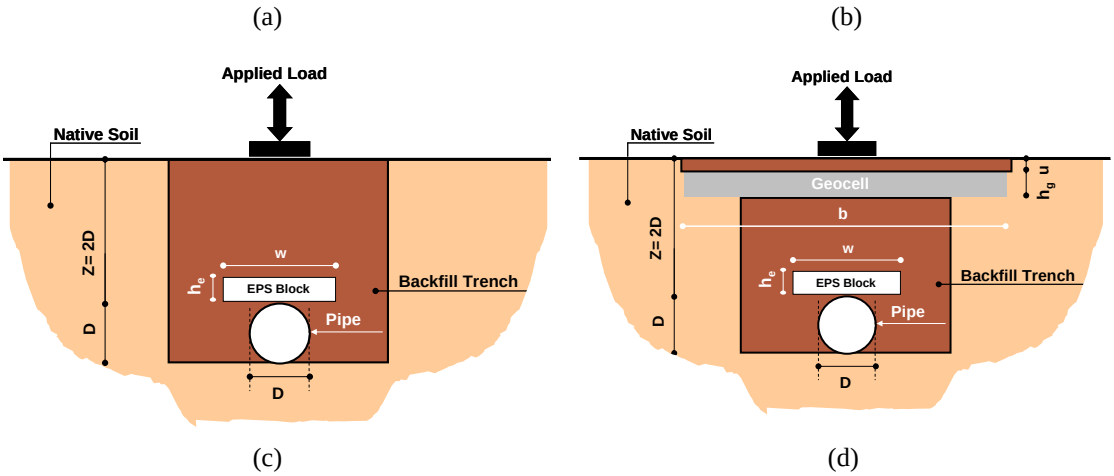

Fig. 8. Schematic view of tests (a) unreinforced backfill without EPS block (b) geocell-reinforced backfill without EPS block (c) unreinforced backfill with EPS block (b) geocell-reinforced backfill with EPS block

809

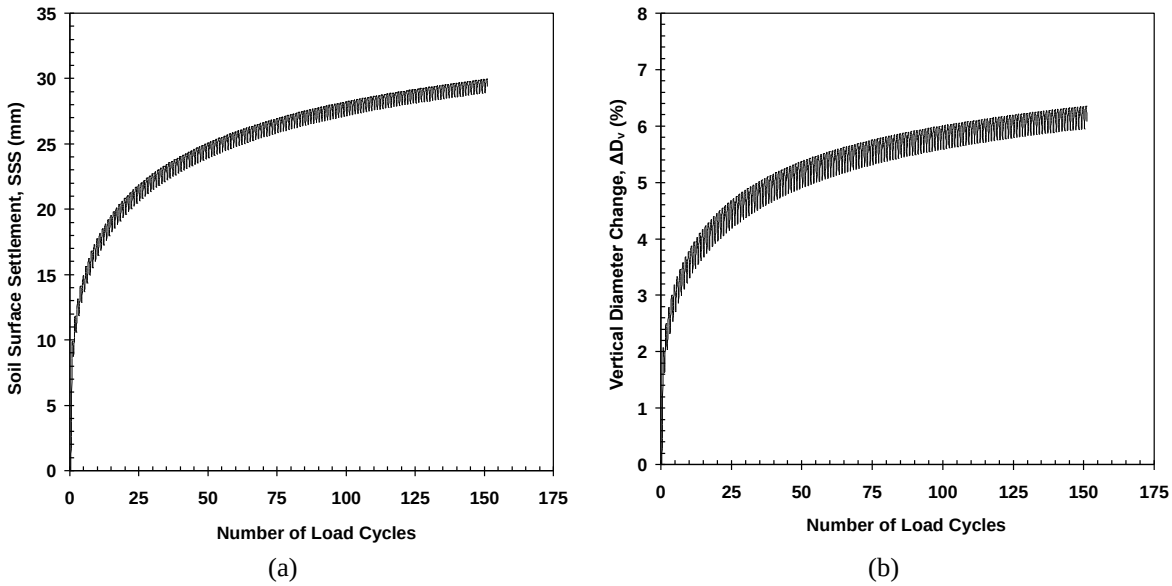

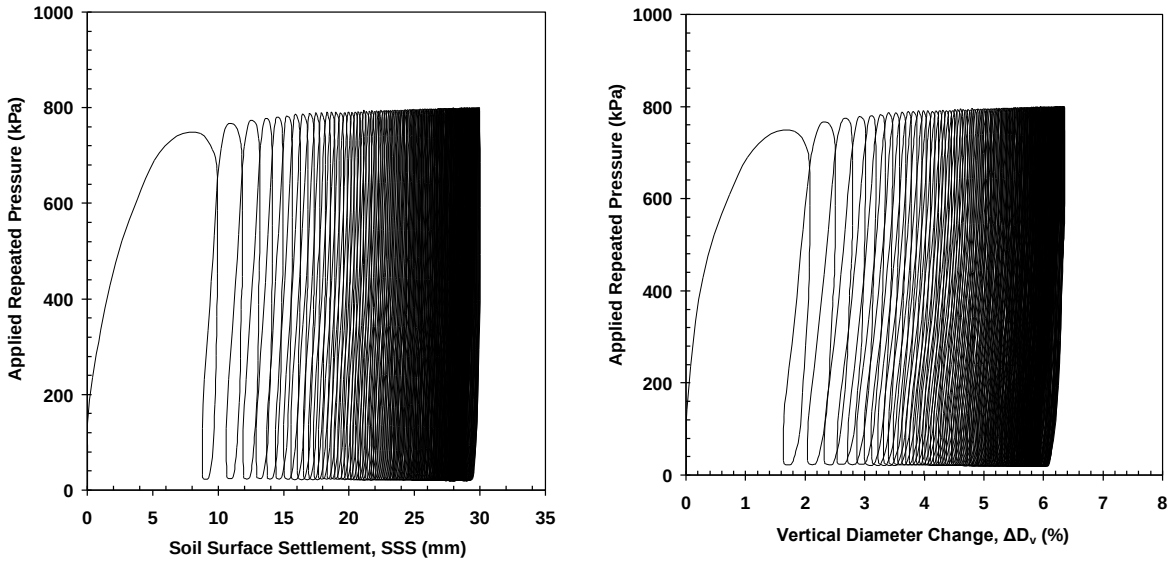

(c) (d)

Fig. 9. Typical trend of (a) SSS with load cycles, (b) ΔD_v with load cycles, (c) hysteresis curve of SSS, (d) hysteresis curve of ΔD_v

810

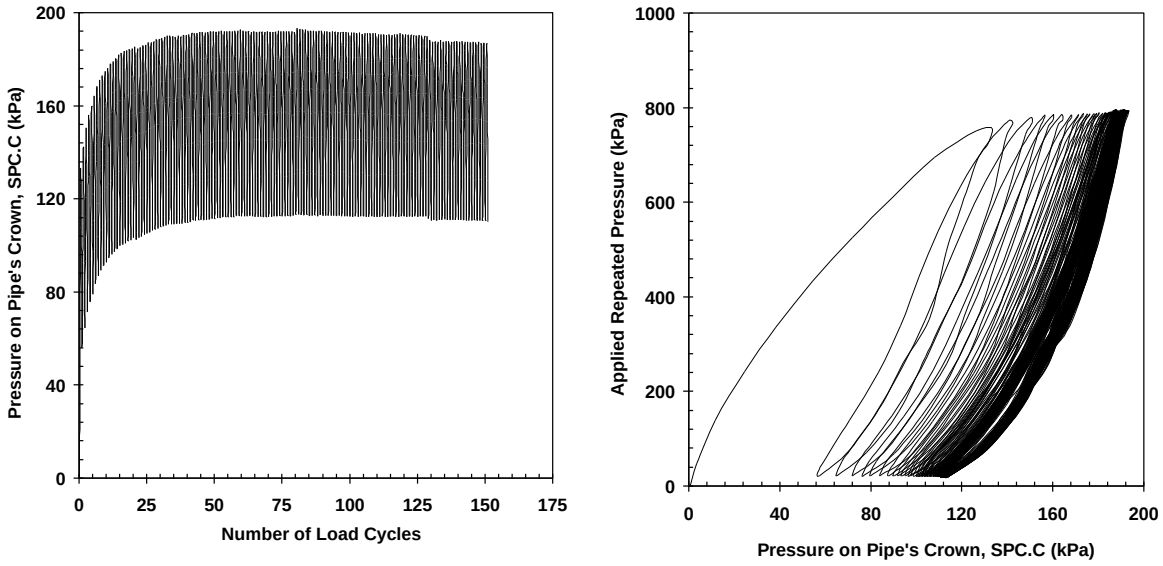

(a) (b)

Fig. 10. Typical trend of (a) transferred pressure on pipe with load cycles, (b) hysteresis curve of transferred pressure

811

812

813

814

815

816

817

818

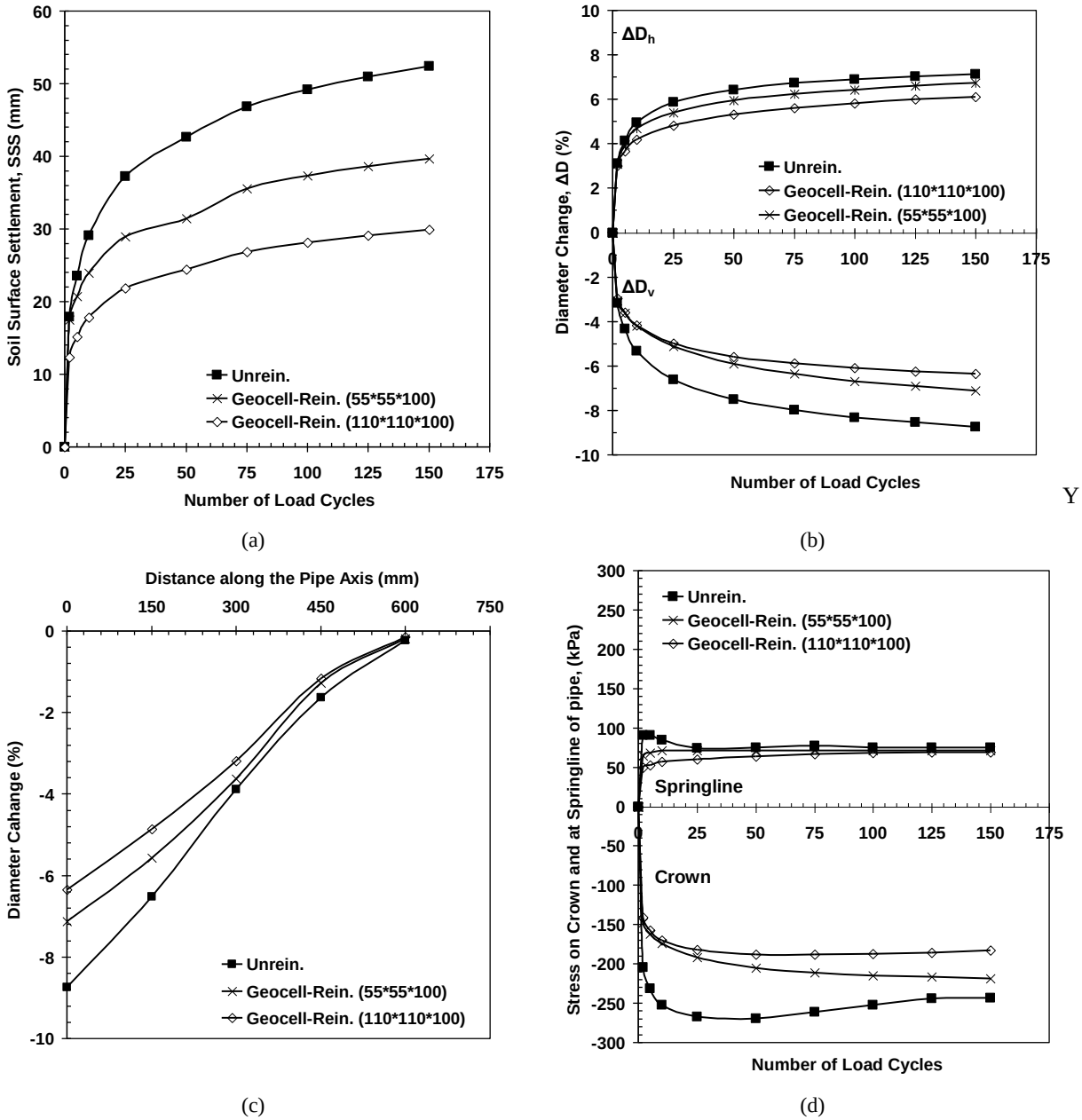

Y

Fig. 11. Comparison between geocell-reinforced and unreinforced installations for (a) SSS, (b) ΔD_v and ΔD_h, (c) pipe deformation in longitudinal axis, and (d) Soil pressure on crown and at springline of pipe (SPC. C and SPC.

S)

819

820

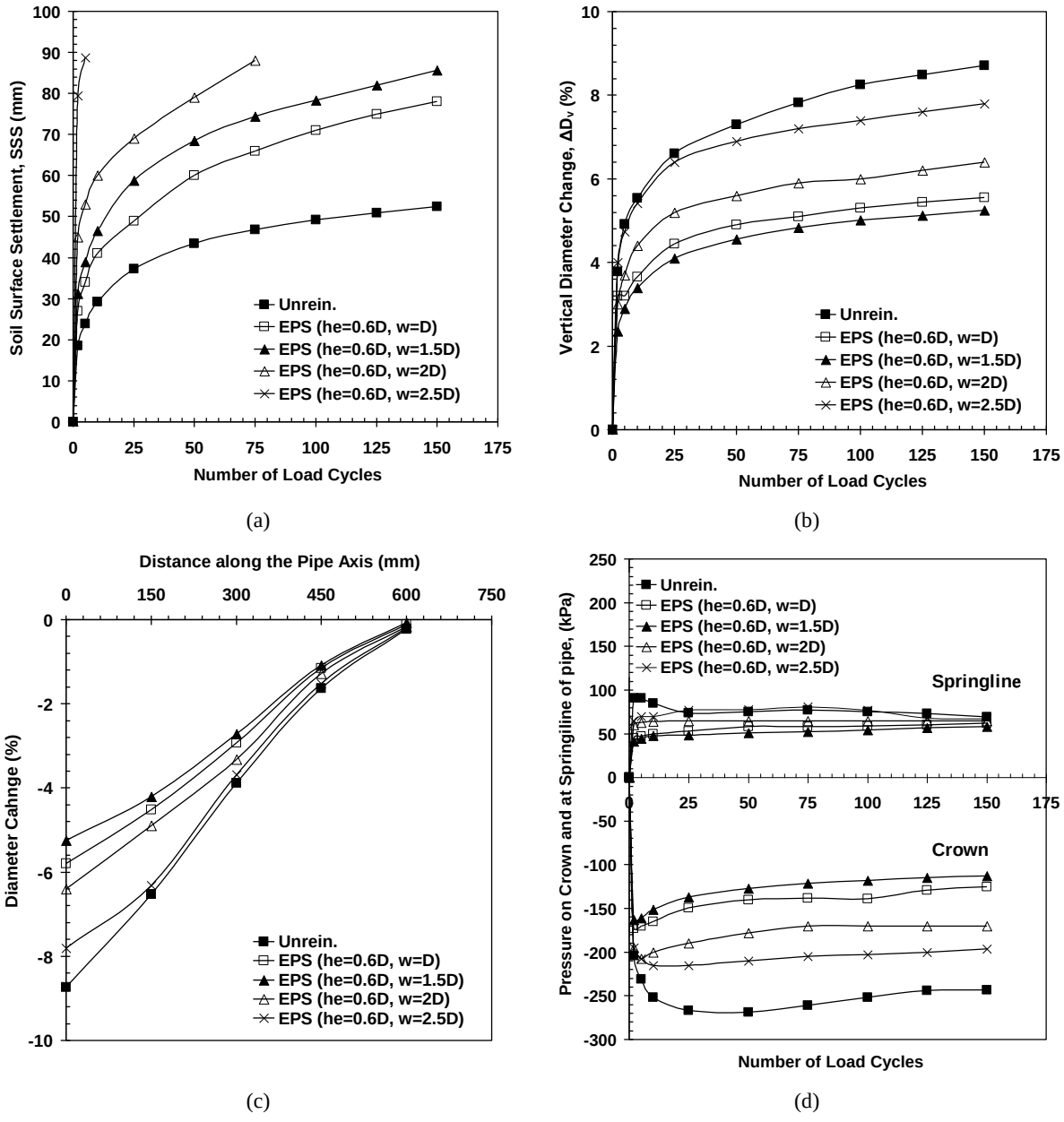

Fig. 12. The effect of EPS block width in unreinforced installation on (a) SSS, (b) ΔD_v, (c) pipe deformation in longitudinal axis, and (d) Soil pressure on crown and at springline of pipe (SPC. C and SPC. S)

821

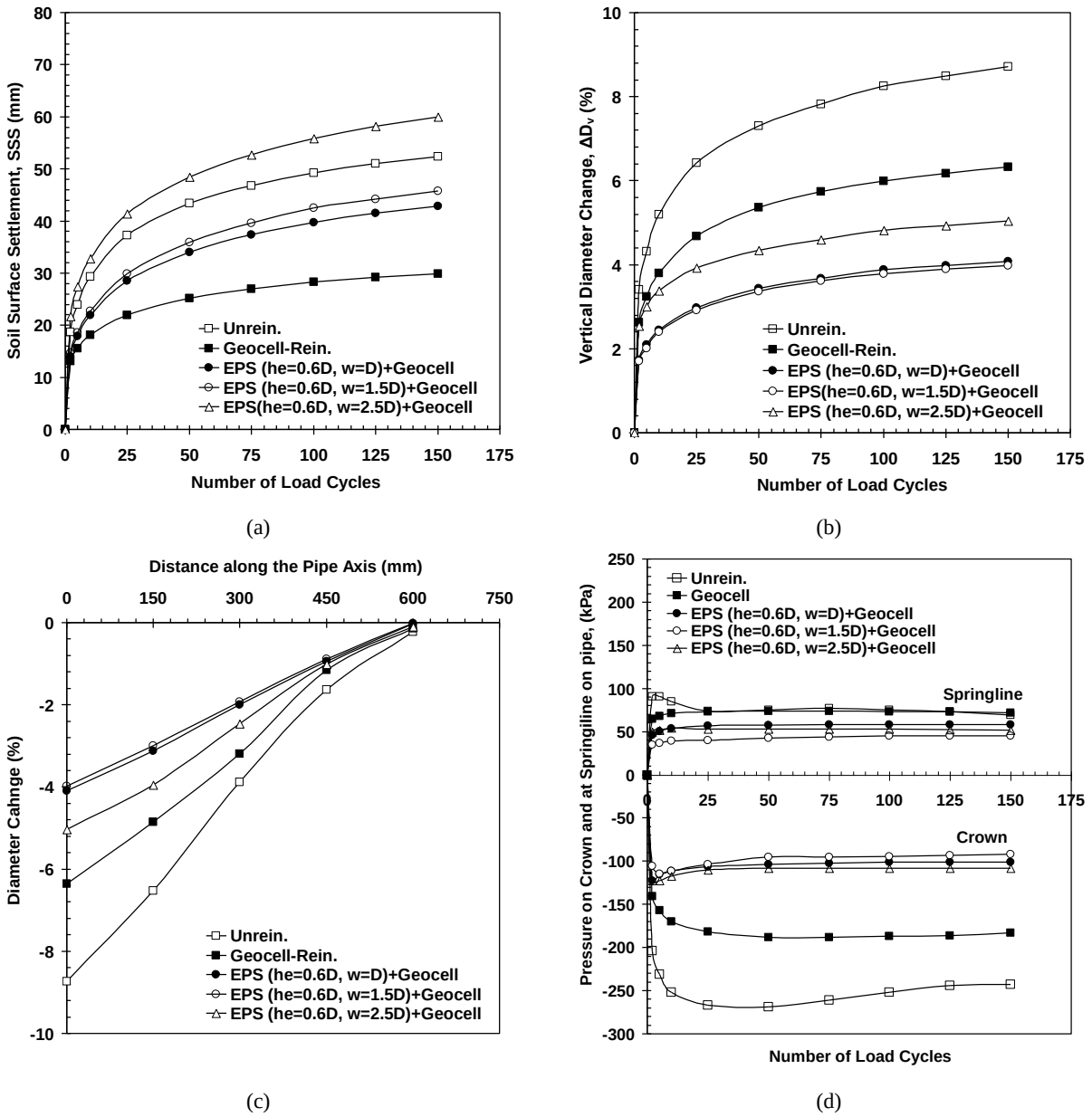

Fig. 13. The effect of EPS block width in unreinforced installation on (a) SSS, (b) ΔD_v, (c) pipe deformation in longitudinal axis, and (d) Soil pressure on crown and at springline of pipe (SPC. C and SPC. S)

822

823

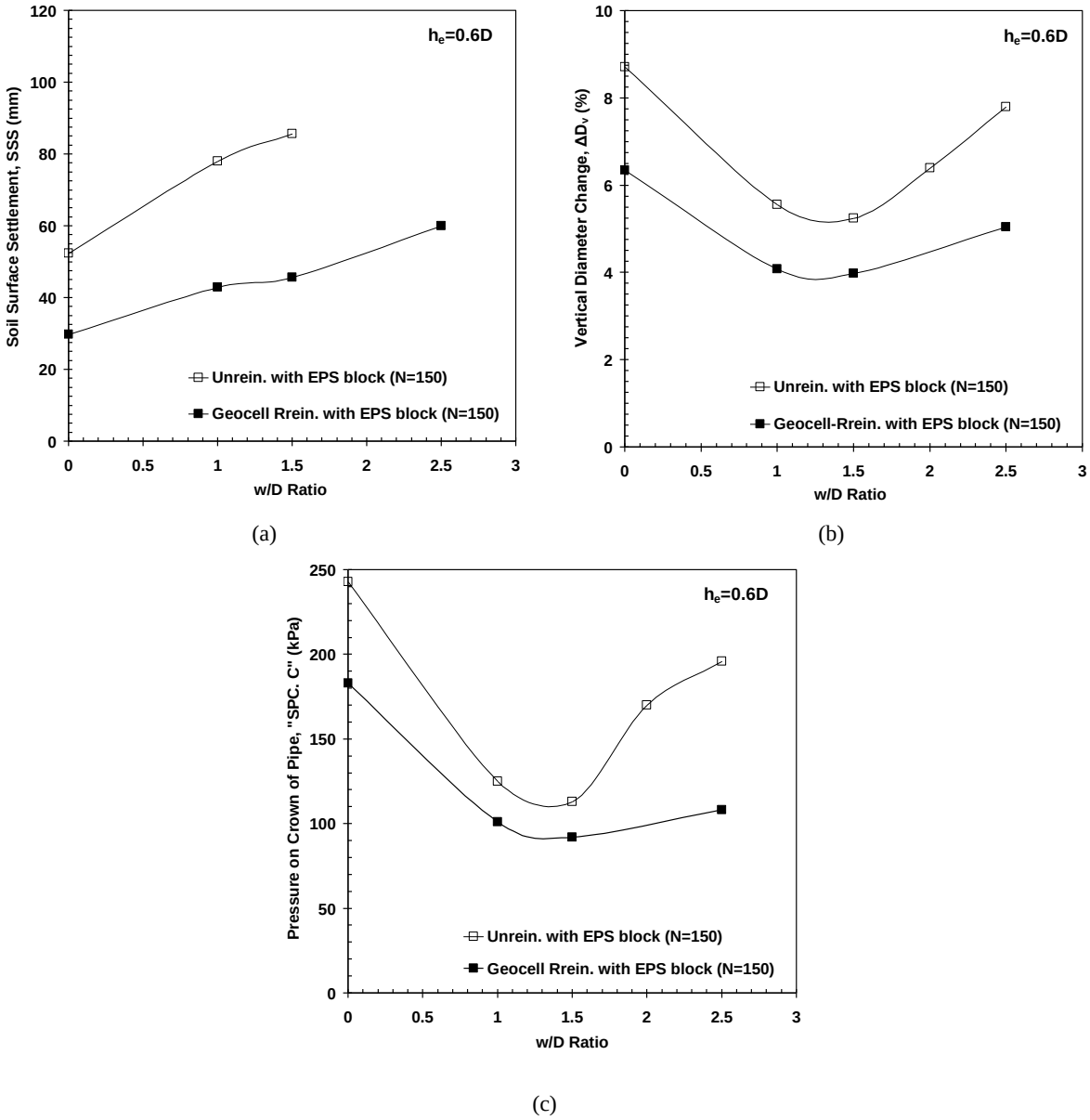

Fig. 14. Variation of (a) SSS, (b) ΔD_v, and (c) pressure on pipe crown with w/D for unreinforced and geocell-reinforced installations (h_e/D=0.6)

824

825

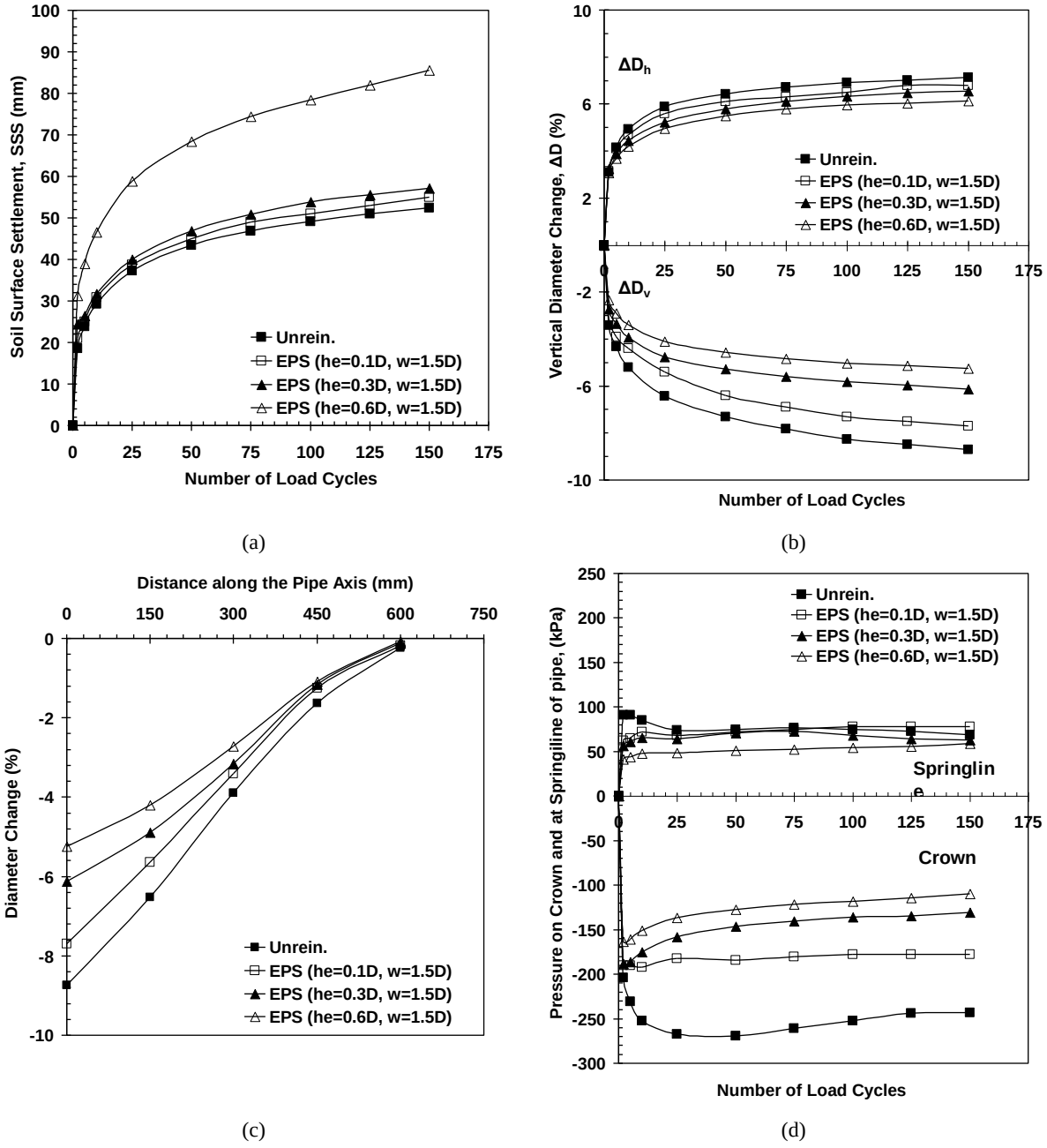

Fig. 15. The effect of EPS block thickness in unreinforced installation on (a) SSS, (b) ΔD_v, and ΔD_h (c) pipe deformation in longitudinal axis, and (d) Soil pressure on crown and at springline of pipe (SPC. C and SPC. S)

826

827

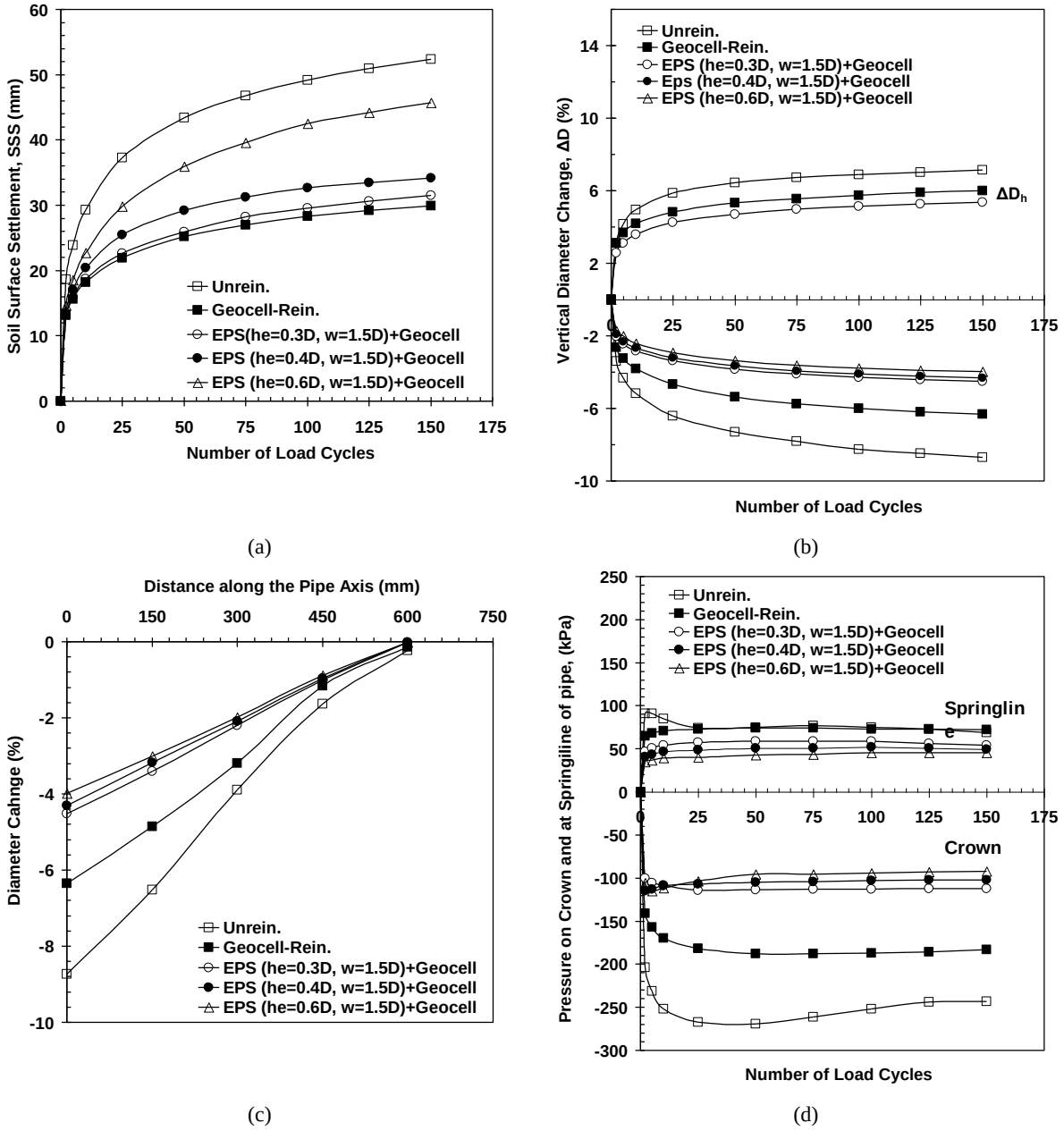

Fig. 16. The effect of EPS block thickness in geocell-reinforced installation on (a) SSS, (b) ΔD_v, and ΔD_h (c) pipe deformation in longitudinal axis, and (d) pressure on crown and at springline of pipe (SPC. C and SPC. S)

828

829

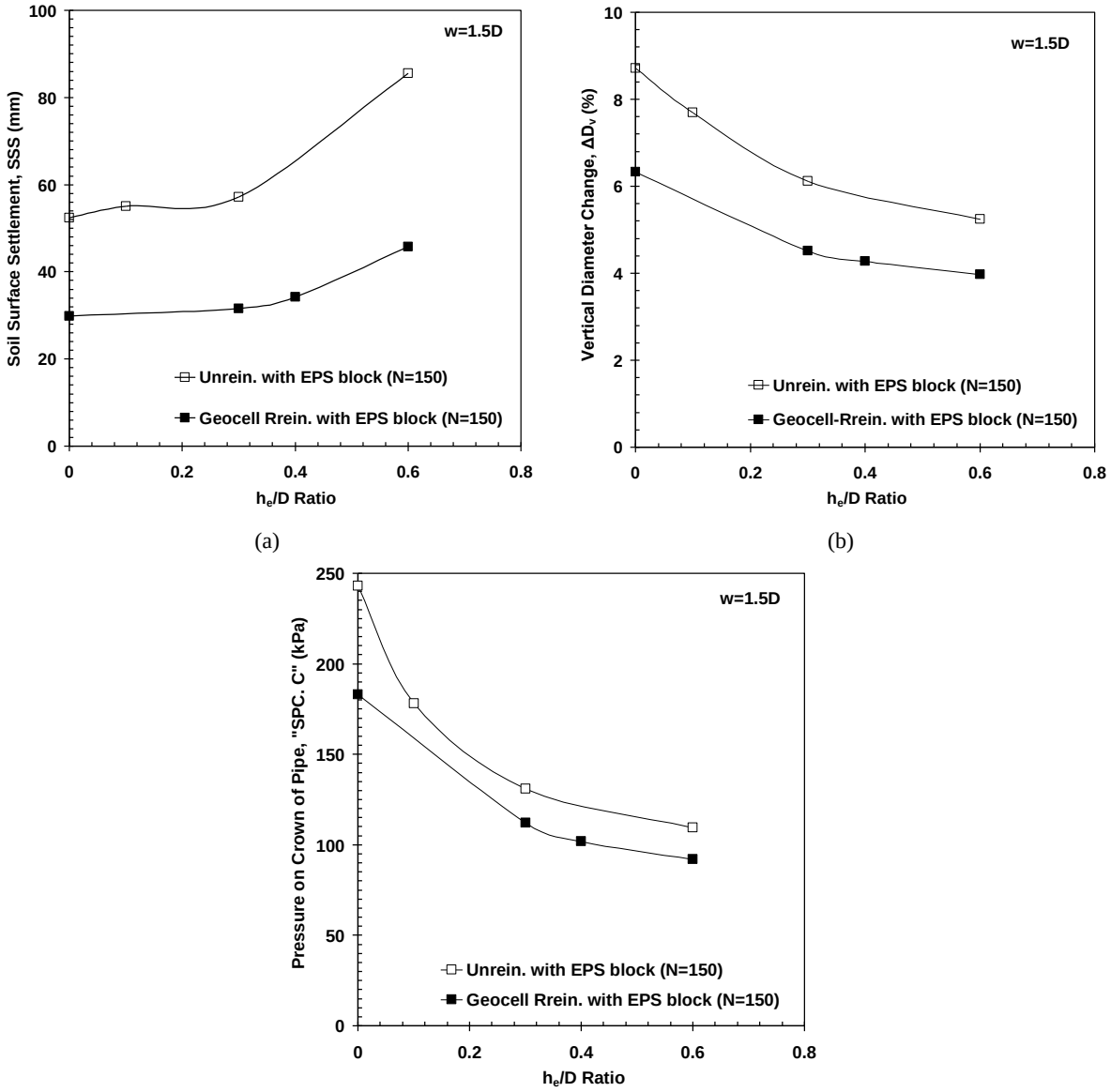

Fig. 17. Variation of (a) SSS, (b) ΔD_v and (c) pressure on pipe crown with h_e/D for unreinforced and geocell-reinforced installations (w/D=1.5)

830
831

Table 1. The engineering properties of the geotextile used in the tests (reported by manufacturer- See acknowledgment)

Description	**Value**
Type of geotextile	Non-woven
Material	Polypropylene
Areal weight (g/m^2)	190
Thickness under 2 kN/m^2 (mm)	0.57
Thickness under 200 kN/m^2 (mm)	0.47
Tensile strength (kN/m)	13.1
Strength at 5% (kN/m)	5.7

Effective opening size (mm)	0.08

Table 2. Densities of soil for unreinforced and geocell-reinforced layers after compaction (ASTM D 1557-12)

Type of layer	Average dry unit weight (kN/m^3)
Unreinforced soil layer above pipe crown	≈18.78*
Unreinforced soil layer in the both sides of the pipe	≈16.2**
Geocell-reinforced layer (110×110×100 mm)	Between 18.2 and 18.4
Geocell-reinforced layer (55×55×100 mm)	Between 17.5 and 17.8

*approximately 92% of maximum dry unit weight – see Sec. 3.1

*approximately 80% of maximum dry unit weight

Table 3. Scheme of the tests on buried pipe and parameters considered (z=2D, D=250 mm)

Test Series	Test Configuration	Reinforcement Status	Geocell Size (mm×mm)	Thickness of EPS Block (h_e)	Width of EPS Block (w)	No. of Tests
1	No EPS Block	Unreinforced	---	---	---	1+1**
2		Geocell-reinforced	50×50	---	---	2+3**
			110×110			
3	EPS Block	Unreinforced	---	***0.6D	D, 1.5D, 2D, 2.5D	4+4**
				0.1D, 0.3D, 0.6D	1.5D	2*+3**
4		Geocell-reinforced	110×110	***0.6D	D, 1.5D, 2.5D	3+3*
				0.3D, 0.4D, 0.6D	1.5D	2*+3**

** Number indicates number in series which includes tests also listed in other rows*

***The tests which were performed two or three times to verify the repeatability of the test data. For example, in test Series 2, a total of 5 tests were performed, including 2 independent tests plus 3 replicates.*

****the tests in which the horizontal diameter changes were not recorded.*

Table 4. The soil surface settlement (SSS), vertical diametric change (ΔD_v), Pressure over pipe for unreinforced and geocell-reinforced installations with and without EPS block at the last cycle of loading

Test condition		No EPS block	With EPS block						
			h_e	0.6D	0.6D	0.6D	0.6D	0.1D	0.3D	0.4D
				w						
				D	1.5D	2D	2.5D	1.5D	1.5D	1.5D
Unreinforced	SSS (mm)	52.42		78.2	85.62	88.2*	88.8**	55.2	57.2	----
	ΔD_v (%)	8.74		5.8	5.25	6.41	7.81	7.71	6.12	----
	Pressure over Pipe (kPa)	243		125	113	170	196	178	131	----
Geocell-reinforced 110×110 mm^2	SSS (mm)	29.91		42.88	45.75	----	60.2	----	31.53	34.21
	ΔD_v (%)	6.35		4.08	3.98	----	5.04	----	4.52	4.31
	Pressure over Pipe (kPa)	183		101	92	----	108	----	112	102

**the SSS value at load cycle of 75*

***the SSS value at load cycle of 5*

835

836

837